Robertson, A.H.F., Emeis, K.-C., Richter, C., and Camerlenghi, A. (Eds.), 1998
Proceedings of the Ocean Drilling Program, Scientific Results, Vol. 160

2. THE MIOCENE/PLIOCENE BOUNDARY IN THE EASTERN MEDITERRANEAN: RESULTS FROM SITES 967 AND 969[1]

Silvia Spezzaferri,[2] Maria B. Cita,[3] and Judith A. McKenzie[2]

ABSTRACT

Continuous sequences developed across the Miocene/Pliocene boundary were cored during Ocean Drilling Project (ODP) Leg 160 at Hole 967A, located on the base of the northern slope of the Eratosthenes Seamount, and at Hole 969B, some 700 km to the west of the previous location, on the inner plateau of the Mediterranean Ridge south of Crete. Multidisciplinary investigations, including quantitative and/or qualitative study of planktonic and benthic foraminifers and ostracodes and oxygen and carbon isotope analyses of these microfossils, provide new information on the paleoceanographic conditions during the latest Miocene (Messinian) and the re-establishment of deep marine conditions after the Messinian Salinity Crisis with the re-colonization of the Eastern Mediterranean Sea in the earliest Pliocene (Zanclean).

At Hole 967A, Zanclean pelagic oozes and/or hemipelagic marls overlie an upper Messinian brecciated carbonate sequence. At this site, the identification of the Miocene/Pliocene boundary between 119.1 and 119.4 mbsf, coincides with the lower boundary of the lithostratigraphic Unit II, where there is a shift from a high content of inorganic and non-marine calcite to a high content of biogenic calcite typical of a marine pelagic ooze. The presence of *Cyprideis pannonica* associated upward with Paratethyan ostracodes reveals that the upper Messinian sequence is complete. The stable isotope composition of *C. pannonica* indicates that this crustacean lived in a Lago Mare environment characterized by brackish water, distinctly different from the marine environment. At Hole 969B, the identification of the Miocene/Pliocene boundary coincides with a marked lithologic change between 97.1 and 97.2 mbsf. The marine sediments directly overlie latest Messinian Lago Mare facies deposits comprising dark gray clay. The presence of planktonic foraminifers associated with brackish water ostracodes in Hole 967A, and with the gray clay in Hole 969B, may indicate temporary incursions of Atlantic water into a fully Lago Mare environment. This interpretation is also supported by the trends in the isotopic composition of the ostracodes and planktonic foraminifers.

After the Messinian Salinity Crisis, benthic foraminifers slowly repopulated the Eastern Mediterranean seafloor during the *Sphaeroidinellopsis* acme event (Biozone MPl1). The gradual ingression of typical deep Atlantic benthic foraminifers, *Parrelloides bradyi* and *P. robertsonianus*, and the presence of *Globorotalia menardii* (planktonic foraminifer) coincident with the boundary between the biozones MPl1 and MPl2 indicate that an efficient connection between the Atlantic Ocean and the Eastern Mediterranean Sea was re-established in this interval.

INTRODUCTION

The paleogeography and paleoceanography of the Mediterranean experienced drastic changes during the latest Miocene (the latest part of the Messinian stage) when this marginal sea lost its connection with the Atlantic Ocean and became temporarily isolated as a result of the interaction of plate motions and glacio-eustatic sea-level changes (Ryan, Hsü, et al., 1973; Hsü, Montadert, et al., 1978). This isolation resulted in a "salinity crisis" of the Mediterranean, whereby the world's ocean lost 6‰ of its salinity because approximately one million cubic kilometers of evaporites were deposited on the floor of the deep Mediterranean basins (Hsü et al., 1973; Ryan, 1973).

The earliest Pliocene transgression (Zanclean stage) documents the re-establishment of open marine conditions in the Mediterranean. This drastic change is observed in both deep-sea settings and land exposures with carbonate pelagic oozes directly overlying Lago Mare deposits, which are characteristic for the latest post-evaporitic Messinian. Sedimentary successions across the Miocene/Pliocene boundary were encountered during Leg 160 in the Eastern Mediterranean at Hole 967A on the Eratosthenes Seamount and Site 969 on the Mediterranean Ridge (Emeis, Robertson, Richter, et al., 1996; Fig. 1).

Previous studies of the Miocene/Pliocene boundary and the significance of the Pliocene transgression after the termination of the Messinian Salinity Crisis date back to the first drilling campaign in the Mediterranean during Deep Sea Drilling Program (DSDP) Leg

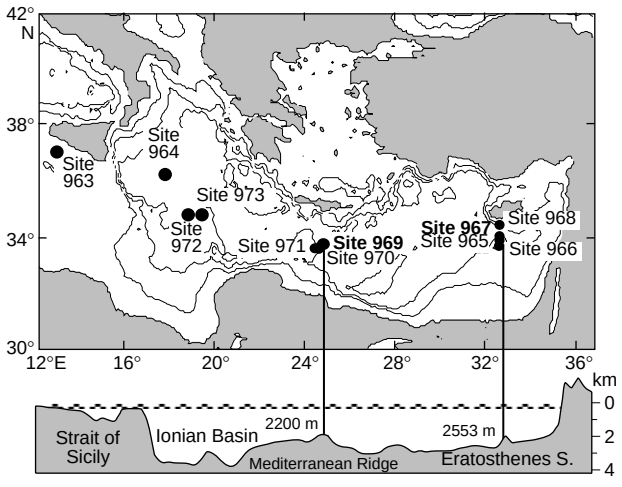

Figure 1. Map of the Eastern Mediterranean showing the locations of Sites 963–973. The depth positions of Sites 967 and 969 are indicated on the topographic profile shown in the inset.

[1]Robertson, A.H.F., Emeis, K.-C., Richter, C., and Camerlenghi, A. (Eds.), 1998. *Proc. ODP, Sci. Results*, 160: College Station, TX (Ocean Drilling Program).

[2]Geologisches Institut, ETH-Zentrum, Sonneggstrasse 5, 8092, Zurich, Switzerland. silvia@erdw.ethz.ch

[3]Dipartimento di Scienze della Terra, Universitá di Milano, Via Mangiagalli 34, 20133, Milano, Italy.

13, and subsequent land studies in Sicily (Ryan, Hsü, et al., 1973; Cita and Ryan, 1973; Cita, 1973b, 1975b; Cita and Gartner, 1973). The first paleomagnetic calibration of the Miocene/Pliocene boundary, providing precise timing of the event, was obtained by Zijderweld et al. (1986) in the Singa Section from Calabria. Subsequent high-resolution stratigraphy research carried out in Sicily and Calabria (Hilgen, 1991; Hilgen and Langereis, 1993) and in the Tyrrhenian ODP Site 652 (McKenzie and Sprovieri, 1990; McKenzie at al., 1988, 1990) indicated that the boundary is isochronous on land (Eraclea Minoa, Rossello Composite, Singa Composite) and in the deep sea, at least in the central Mediterranean. The Miocene/Pliocene boundary as defined by Cita (1975a) at the base of the Zanclean at Capo Rossello is not yet formalized in a strictly chronostratigraphic sense. A global stratotype section and point (GSSP) has been recently proposed for a section in Morocco (Benson and Hodell, 1994), which has the Miocene/Pliocene boundary located in a position older than has been consistently used in the last 20 years.

The present study was undertaken using a multidisciplinary approach to investigate the sedimentary sequences obtained from the newest ODP drill sites in the Eastern Mediterranean. We propose to evaluate the stratigraphic events across the Miocene/Pliocene boundary in this region and compare them with sequences from the Western Mediterranean. Ultimately, the goal is to test the synchroneity of the events on a basin-wide scale.

MATERIALS AND METHODS

High-resolution sampling of the sediments from Holes 967A (Fig. 2) and 969E was done for this study aboard the *JOIDES Resolution* at closely spaced intervals of approximately 10–50 cm throughout the latest Miocene Lago Mare sequence and the MPl1 and MPl2 Zones. Hole 969B was sampled postcruise at the Bremen Core Repository (Fig. 3).

The sample volume was ~5–10 cm^3. Samples were soaked in distilled water, washed under running water through 40- to 150-µm, 151- to 250-µm, and >250-µm sieves. The three size fractions obtained were then dried at room temperature and weighed to determine eventual sorting and/or degree of dissolution (Premoli Silva et al., 1993; Spezzaferri, 1995). Samples were then re-assembled and dry-sieved through the 125-µm mesh sieve for quantitative study. This was done to facilitate the comparison with previous studies (McKenzie et al., 1990: Sprovieri, 1993). Three hundred specimens of planktonic foraminifers were counted for each sample for the interval spanning the MPl1 to MPl2 biozones. No planktonic foraminifers were counted for Hole 969E where the oldest part of the Zanclean was not observed.

The calcium carbonate content was measured in bulk samples using a Dichter-Freeling calcimeter. Three to ten specimens of *Oridorsalis stellatus* and 20 to 30 specimens of *Globigerinoides obliquus* were picked from each sample for stable isotope analysis. Oxygen and carbon isotopes were measured using a PRISM Mass Spectrometer in the Stable Isotope Laboratory of the Geological Institute, ETH-Zurich. The isotope data, corrected following the procedure of Craig (1957), modified for a triple collector and relative to the international standard Pee Dee Belemnite (PDB), together with the data of weight of size fractions, percent abundance of planktonic foraminifers and carbonate content as well as the depth below seafloor (mbsf) and the revised composite depth (rmcd), are given in Tables 1–3.

BIOSTRATIGRAPHIC RESULTS

Site 967 (Eratosthenes Seamount)

Although Site 967 on the Eratosthenes Seamount was planned for tectonic objectives only, it proved to be an exceptional location for studying the Miocene/Pliocene boundary problem. Hole 967A is located on the lower northern slope of the Eratosthenes Seamount (34°04.098′N, 32°43.523′E, water depth of 2553 m, penetration of 141.3 m). The advanced piston corer (APC) was used down to 123.3 mbsf. The extended core barrel (XCB) was used down to 141.3 mbsf. Recovery throughout was close to 100%. The upper part of the sedimentary sequence comprises about 100 m of Pliocene–Quaternary nannofossil oozes and nannofossil clay with numerous sapropels. The lower part comprises slightly brecciated and indurated carbonates.

The investigated interval includes Core 160-967A-13H downward. In the Leg 160 *Initial Reports* volume (Emeis, Robertson, Richter, et al., 1996), the sedimentary section is described in the barrel sheets as lower Pliocene until the upper part of Core 160-967A-15X, but this is not the case. Strong coring disturbance is notable in Core 160-967A-13H starting from Section 160-967A-13H-4 (see Fig. 2 where the locations of the 29 investigated samples are shown). No typical Pliocene age assemblages are recorded lower than Section 160-967A-13H-3.

Planktonic and benthic foraminiferal assemblages, plus ostracodes, indicate a variety of ages and environments. Of special interest is the recorded occurrence of the so-called Lago Mare biofacies typical of the latest post-evaporitic Messinian. Notably, at this location no Messinian evaporites were cored. The pore-water profiles of salinity, chlorite, and sodium, however, reach values almost twice those of seawater, suggesting that evaporites or an evaporite brine may be present deeper (>150 mbsf) downhole (Emeis, Robertson, Richter, et al., 1996). This interpretation is also supported by the downhole logging data (Major et al., Chap. 38, this volume). Age determination for the lower Pliocene sequences identified in this study are based on planktonic foraminiferal zonal schemes proposed by Cita (1975b) and amended by Sprovieri (1992, 1993).

Planktonic Foraminifers

Planktonic foraminifers range in abundance from absent in the lower part of the section to dominant. They consist of diversified and poorly to well-preserved lower Pliocene (Zanclean) faunas.

Zone MPl2 is identified from Sample 160-967A-12H-CC, 42–44 cm, to 13H-2, 19–21 cm. Planktonic foraminiferal assemblages include common to abundant *Orbulina universa, Globigerinoides obliquus, G. quadrilobatus, G. sacculifer, G. trilobus, Globorotalia margaritae, G. scitula, Globigerina falconensis, Globigerinita juvenilis, G. glutinata, Neogloboquadrina acostaensis* dextral and sinistral, *Zeaglobigerina woodi, Turborotalita quinqueloba*, and the *Z. nepenthes* group. Minor components are *Globigerina bulloides, Globigerinoides ruber, Sphaeroidinellopsis* group (which includes *S. seminulina, S. subdehiscens*, and *S. kochi*), and *Zeaglobigerina decoraperta.* Specimens belonging to the *Globorotalia menardii* group were observed across the MPl1/MPl2 zonal boundary in Samples 160-967A-13H-2, 19–21 cm, and 13H-2, 135–37 cm (Pl. 1, Fig. 12).

Zone MPl1 is identified from Sample 160-967A-13H-2, 35–37 cm, to 13H-4, 78–80 cm, with a total thickness of 3.43 m. Planktonic foraminiferal assemblages are similar to those observed in Zone MPl2, except for the absence of *G. margaritae.* The *Sphaeroidinellopsis* acme event is identified from Sample 160-967A-13H-3, 25–27 cm, to 13H-3, 113–115 cm (Table 4).

From Samples 160-967A-13H-4, 25–27 cm, to 13H-4, 78–80 cm, rare large-sized planktonic foraminifers occur together with a dwarf fauna predominantly composed of *T. quinqueloba.* This assemblage is interpreted as the lowermost Zanclean assemblage, predating the *Sphaeroidinellopsis* acme event.

Messinian sediments were recovered from Sample 160-967A-13H-4, 109–111 cm, to 16X-1, 84–86 cm. These sediments are characterized by mixed Eocene, Oligocene, and middle Miocene planktonic foraminiferal assemblages (Table 5). Reworked specimens in-

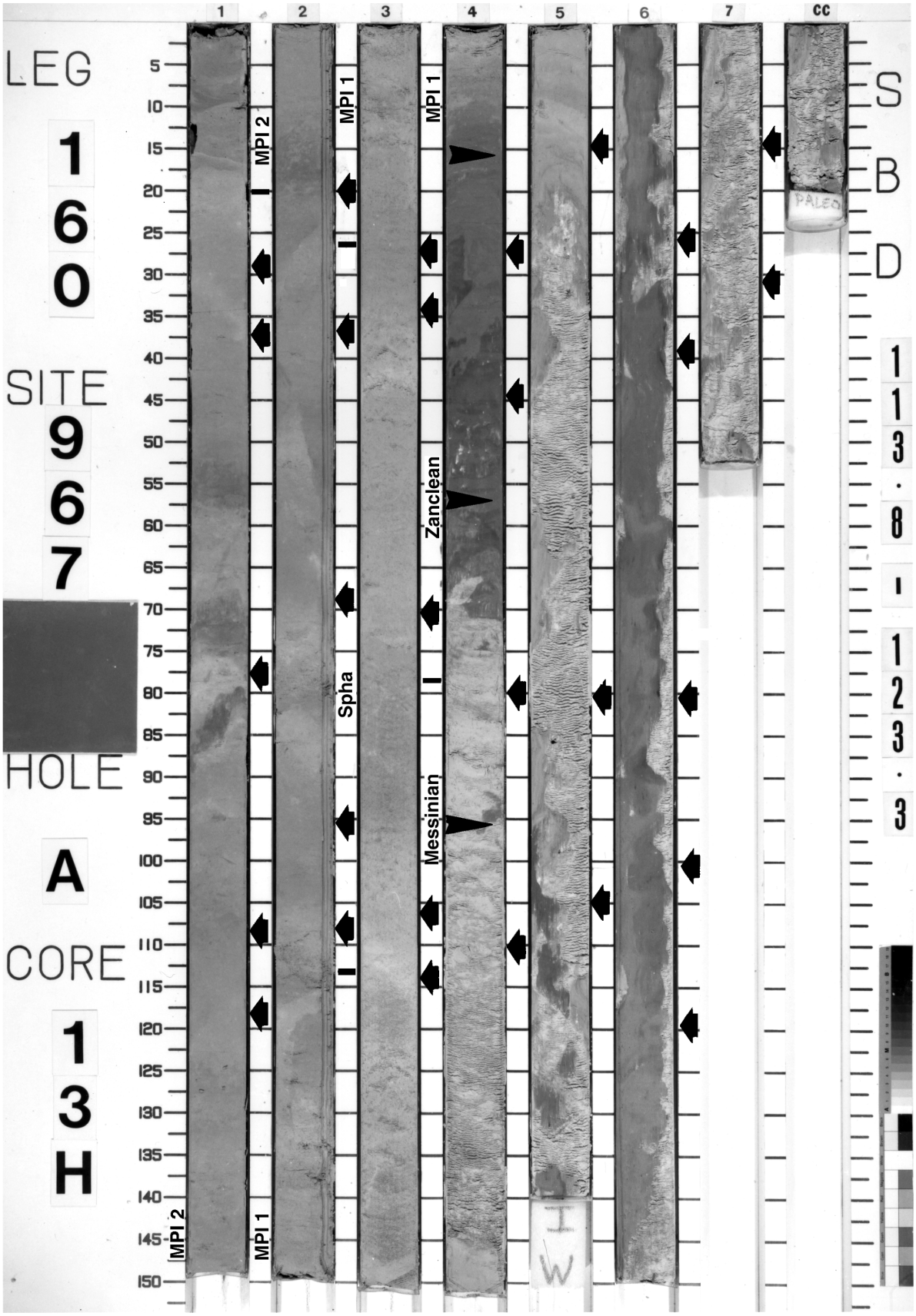

Figure 2. Photograph of Core 160-967A-13H, showing the location of the 29 investigated samples.

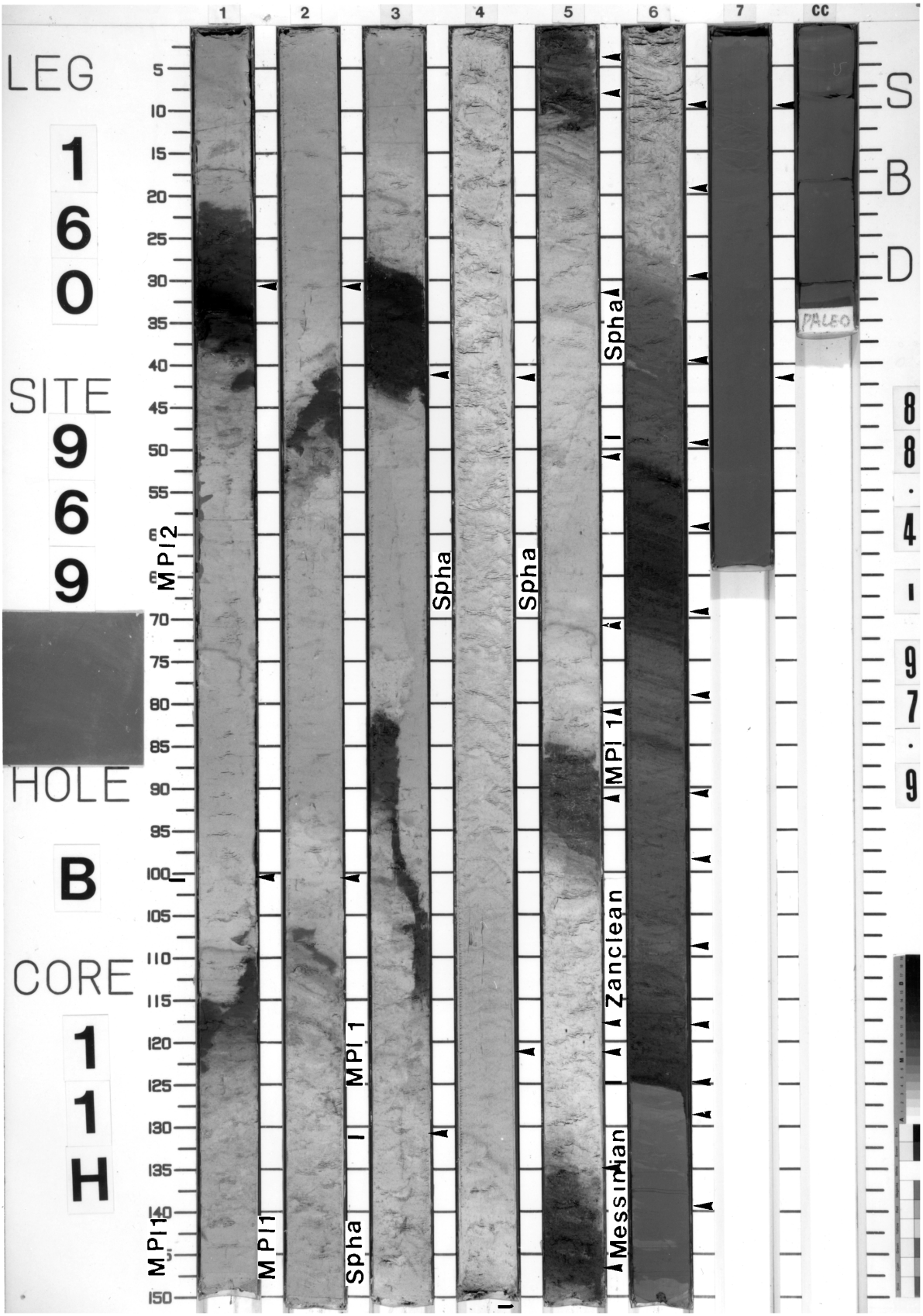

Figure 3. Photograph of Core 160-969B-11H, showing the location of the 36 investigated samples.

Table 1. Abundance of size fractions (>151 µm, 40–151 µm, and < 40 µm), calcium carbonate content, and stable isotopes of *G. obliquus, O. stellatus*, and *C. pannonica* plotted vs. mbsf and rmcd for Hole 967A.

Core, section, interval (cm)	Depth (mbsf)	Depth (rmcd)	$CaCO_3$ (wt%)	Size fraction >151 µm	Size fraction 40–151 µm	Size fraction <40 µm	Planktonic foraminifers $\delta^{13}C$	Planktonic foraminifers $\delta^{18}O$	Benthic foraminifers $\delta^{13}C$	Benthic foraminifers $\delta^{18}O$	Ostracodes *C. pannonica* $\delta^{13}C$	Ostracodes *C. pannonica* $\delta^{18}O$
160-967A-												
12H-CC	113.450	120.310	—	—	—	—	0.995	–0.527	–0.674	1.616	—	—
13H-1, 27-29	114.070	122.960	55.260	1.980	1.630	0.940	1.259	0.109	–0.982	1.821	—	—
13H-1, 35-37	114.150	123.060	55.380	1.903	1.130	0.815	1.166	0.259	—	—	—	—
13H-1, 77-79	114.570	123.410	60.780	2.890	1.380	1.010	1.518	–0.200	–0.807	1.614	—	—
13H-1, 107-109	114.870	123.690	48.790	1.274	1.376	0.713	1.316	–0.808	–0.826	1.395	—	—
13H-1, 117-119	114.970	123.740	66.950	2.080	1.610	1.070	1.375	–0.076	–0.365	1.273	—	—
13H-2, 19-21	115.490	124.170	48.150	2.670	1.650	0.920	1.352	–0.176	–0.285	1.313	—	—
13H-2, 35-37	115.650	124.320	54.060	2.585	1.856	1.638	1.106	–0.841	–0.620	1.408	—	—
13H-2, 67-69	115.970	124.610	59.210	4.540	0.230	6.410	1.306	–0.100	–0.482	1.439	—	—
13H-2, 94-96	116.240	124.860	62.360	2.420	2.050	0.780	1.125	–0.260	–0.635	1.500	—	—
13H-2, 106-108	116.360	124.970	58.020	3.293	3.977	5.249	1.549	–0.586	–0.152	1.500	—	—
13H-3, 25-27	117.050	125.600	63.150	3.590	1.480	0.250	1.249	–0.167	–0.769	1.129	—	—
13H-3, 33-35	117.130	125.680	63.290	3.299	2.108	0.733	1.694	–0.554	0.330	0.062	—	—
13H-3, 69-71	117.490	126.010	73.810	5.790	3.030	1.380	1.611	–1.216	–0.527	1.244	—	—
13H-3, 105-107	117.850	126.340	67.910	6.270	4.478	1.827	1.726	–1.143	–0.612	1.383	—	—
13H-3, 113-115	117.930	126.410	71.050	4.510	2.310	1.280	1.819	–0.315	–0.027	1.547	—	—
13H-4, 25-27	118.500	126.950	21.310	0.150	0.150	0.450	—	—	—	—	—	—
13H-4, 43-45	118.730	127.110	23.730	0.000	8.398	10.575	—	—	—	—	—	—
13H-4, 78-80	119.080	127.320	87.230	0.000	0.290	0.290	—	—	—	—	—	—
13H-4, 109-111	119.390	127.500	85.710	0.080	0.170	0.080	—	—	—	—	—	—
13H-5, 13-15	119.930	127.830	66.230	0.140	1.430	3.710	—	—	—	—	–1.549	–3.040
13H-5, 79-81	120.590	128.490	84.930	0.240	0.480	0.240	—	—	—	—	–0.929	–2.593
13H-5, 103-105	120.830	128.730	56.880	0.107	0.215	1.075	—	—	—	—	—	—
13H-6, 24-26	121.540	129.440	48.790	1.642	3.727	2.653	0.940	–2.323	—	—	–1.800	–3.638
13H-6, 37-39	121.670	129.570	20.250	0.120	0.120	0.120	—	—	—	—	—	—
13H-6, 79-81	122.090	129.990	26.490	0.370	0.370	7.440	1.188	–1.648	—	—	—	—
13H-6, 99-101	122.290	130.190	70.910	0.390	3.980	0.390	0.921	–1.740	—	—	–0.499	–3.221
13H-6, 117-119	122.470	130.870	19.780	6.601	4.950	0.825	0.992	–1.698	—	—	–2.097	–3.142
13H-7, 12-14	122.920	131.320	65.930	0.203	1.464	1.993	—	—	—	—	–0.598	–3.264
13H-7, 29-31	123.090	131.490	82.590	1.760	2.460	1.580	—	—	—	—	–0.570	–3.385
14X-1, 50-52	123.800	137.570	88.330	13.220	5.841	1.155	—	—	—	—	–1.081	–3.662
14X-1, 54-57	123.840	137.670	65.450	11.580	3.580	1.510	—	—	—	—	–0.832	–3.931
14X-1, 72-75	124.020	138.136	76.220	17.560	6.350	1.077	—	—	—	—	—	—
14X-1, 101-103	124.310	138.890	92.500	38.370	3.369	1.987	—	—	—	—	—	—
14X-1, 119-122	124.490	139.249	89.610	1.280	0.560	0.210	—	—	—	—	—	—
14X-2, 21-23	125.020	140.700	56.660	14.160	2.695	1.888	—	—	—	—	–1.966	–2.416
14X-2, 114-116	125.940	143.098	86.660	1.206	0.469	0.000	—	—	—	—	–1.331	–3.350
14X-3, 40-42	126.700	145.046	90.000	0.197	0.413	1.329	—	—	—	—	—	—
14X-3, 124-126	127.540	147.368	80.000	0.000	0.362	0.587	—	—	—	—	—	—
14X-4, 14-16	127.940	148.370	83.330	0.609	1.160	1.044	—	—	—	—	—	—
14X-4, 120-123	129.000	150.700	57.500	0.958	0.243	0.343	—	—	—	—	—	—
14X-5, 19-21	129.490	151.716	62.500	5.507	3.452	2.670	—	—	—	—	—	—
14X-5, 97-100	130.270	153.427	64.160	22.870	4.451	1.432	—	—	—	—	—	—

crease in abundance toward the bottom of the sequence (from Sample 160-967A-13H-7, 12–14 cm, down to the terminal depth). Several samples from 160-967A-13H-4, 109–111 cm, down to Core 160-967A-15X, contain a planktonic foraminiferal assemblage that includes *G. obliquus*, *G. quadrilobatus*, *O. universa*, and dominant dwarf forms (*T. quinqueloba*) associated with brackish water ostracodes. A peak of major abundance of these forms is observed from Sample 160-13H-6, 37–39 cm, to 13H-6, 79–81 cm (Fig. 4; Table 5). The attribution of these sediments to the Messinian is based on (1) the principle of stratigraphic superposition, and (2) the occurrence of typical Messinian brackish ostracodes with intact bivalve which are occasionally recorded from Sample 160-13H-4, 109–111 cm, to as far down as Section 160-967A-15X-4.

Benthic Foraminifers

Benthic foraminifer assemblages are well preserved and well diversified throughout Zone MPl2 and part of Zone MPl1 above the *Sphaeroidinellopsis* acme event. Species diversity varies from 9 to 32 species per sample, with an average of 22 (Table 6). Assemblages include *Gyroidinoides laevigatus, Oridorsalis stellatus, Siphonina reticulata, Uvigerina pygmaea, Globocassidulina subglobosa,* and *Pleurostomella alternans.* Minor components include *Martinottiella perparva, M. communis, Karreriella bradyi, Valvulineria marmorea,* and *Brizalina punctata.* Deep Atlantic species *Parrelloides bradyi* and *P. robertsonianus* (Hasegawa et al., 1990; McKenzie et al., 1990; R. Sprovieri, pers. comm., 1996) are observed from the termination of the *Sphaeroidinellopsis* acme event (Sample 160-967A-13H-2, 106–108 cm) upward (Plates 1–2). Species diversity and abundance of benthic foraminifers decrease from Sample 160-967A-13H-3, 25–27 cm, down to 13H-3, 113–115 cm. The species present in this interval include *O. stellatus. G. laevigatus, G. subglobosa,* and *P. quadriloba.* Messinian sediments yield a very poor benthic foraminiferal assemblage, which consists of *Ammonia tepida* and rarely *Elphidium* sp. (Table 5; Pl. 3, Figs. 1a–c)

Ostracodes

Ostracodes are present in Messinian sediments (Pl. 3). *Cyprideis pannonica,* interpreted and described in previous studies in the Eastern Mediterranean deep-sea record as brackish forms (Benson, 1978; Cita et al., 1978), is observed from Sample 160-967A-13H-4, 109–111 cm, to 15X-4, 6–8 cm. Paratethyan brackish ostracodes probably belonging to the species *Loxoconca diaffarovi* (Cita et al., 1980) are observed in Sample 160-967A-13H-4, 109–111 cm. These brackish ostracodes are considered in situ as shown by the occurrence of several specimens with the valves still closed.

Site 969 (Mediterranean Ridge)

The Mediterranean Ridge drill site was planned to reconstruct the paleoceanographic evolution of the Eastern Mediterranean, and, consequently, multiple holes were drilled. Aboard, only Hole 160-969A was biostratigraphically investigated and sampled. Later, Hole 160-

Table 2. Abundance of size fractions (>151 µm, 40–151 µm, and <40 µm), calcium carbonate content, and stable isotopes of *G. obliquus* and *O. stellatus* plotted vs. mbsf and rmcd for Hole 969B.

Core, section, interval	Depth		$CaCO_3$	Size fraction			Planktonic foraminifers		Benthic foraminifers	
(cm)	(mbsf)	(rmcd)	(wt%)	>151 µm	40–151 µm	<40 µm	$\delta^{13}C$	$\delta^{18}O$	$\delta^{13}C$	$\delta^{18}O$
160S-969B-										
11H-1, 31-33	88.720	123.857	47.110	0.240	0.130	0.050	—	—	—	—
11H-1, 100-102	89.410	124.508	82.230	0.007	1.460	0.950	1.694	–0.671	–0.771	1.219
11H-2, 30-32	90.220	124.959	70.250	0.170	1.600	0.980	—	—	–0.626	1.354
11H-2, 100-102	90.910	125.614	82.230	0.040	0.170	0.060	—	—	–1.716	0.998
11H-3, 40-42	91.810	125.711	69.420	0.120	0.060	0.040	—	—	—	—
11H-3, 130-132	92.710	126.924	84.030	0.070	1.550	0.960	1.724	–0.776	–0.560	0.859
11H-4, 40-42	93.310	127.268	92.440	0.340	2.790	1.350	1.580	–0.434	–0.680	1.424
11H-4, 120-122	94.110	127.719	71.850	0.210	1.920	0.890	1.579	–0.604	–0.773	0.894
11H-5, 3-5	94.430	127.980	75.260	15.270	6.750	0.190	1.460	–1.497	—	—
11H-5, 7-9	94.480	128.010	84.030	0.970	1.700	0.510	1.478	–1.192	1.617	–0.116
11H-5, 30-32	94.710	128.140	89.080	0.300	2.480	1.300	—	—	—	—
11H-5, 50-52	94.910	128.270	68.340	4.540	1.870	1.130	1.519	–0.230	–0.637	1.511
11H-5, 70-72	95.110	128.380	73.860	0.710	2.350	1.120	1.916	–0.847	–0.925	0.852
11H-5, 80-82	95.210	128.450	71.120	6.230	4.590	1.250	1.282	–0.914	1.299	0.948
11H-5, 91-92	95.310	128.520	80.500	0.900	1.100	1.490	1.781	–1.270	—	—
11H-5, 117-119	95.580	128.730	89.630	0.730	3.120	1.250	1.976	–0.549	–0.979	1.018
11H-5, 120-122	95.610	128.740	79.100	4.680	2.380	0.960	1.840	–1.260	–0.890	1.396
11H-5, 145-147	95.860	129.010	83.400	1.850	5.390	2.030	1.793	–1.312	—	—
11H-6, 9-10	95.990	129.140	75.400	5.900	1.610	0.530	1.314	–0.073	—	—
11H-6, 19-20	96.090	129.240	73.780	4.140	0.460	0.460	1.324	–0.265	—	—
11H-6, 29-30	96.190	129.340	67.290	7.420	4.770	1.060	1.445	–0.192	—	—
11H-6, 39-40	96.290	129.440	71.810	3.160	1.580	0.520	1.592	–0.724	—	—
11H-6, 49-50	96.390	129.540	39.720	14.660	2.820	0.560	1.592	–0.834	—	—
11H-6, 59-60	96.490	129.640	81.810	10.840	4.330	2.160	1.535	–1.213	—	—
11H-6, 69-70	96.590	129.740	70.540	23.150	5.140	0.850	1.411	–1.065	—	—
11H-6, 79-80	96.690	129.840	85.130	4.520	1.690	0.560	1.689	–0.390	—	—
11H-6, 90-91	96.800	129.950	72.970	4.040	0.510	0.510	1.593	–0.171	—	—
11H-6, 98-99	96.880	130.030	69.090	3.390	1.930	0.960	1.725	–0.323	—	—
11H-6, 108-109	96.960	130.130	74.540	3.630	1.810	0.450	1.630	–0.988	—	—
11H-6, 117-118	97.070	130.220	74.590	7.680	5.760	1.280	1.352	–1.401	—	—
11H-6, 124-126	97.140	130.300	50.910	7.180	2.780	0.920	1.348	–1.468	—	—
11H-6, 128-129	97.180	130.330	13.780	1.510	0.000	0.750	—	—	—	—
11H-6, 139-140	97.290	130.440	12.970	1.380	0.690	0.690	0.857	–1.681	—	—
11H-7, 8-10	97.490	130.640	16.000	0.062	0.240	2.560	1.274	–1.293	—	—
11H-7, 40-42	97.810	130.960	14.000	0.000	0.070	0.035	0.174	0.282	—	—

969E was sampled in detail to fulfill the sample request aimed to reconstruct the Miocene/Pliocene boundary sequence. The study was performed, but a clear gap has been documented in Section 160-969E-11H-6, 25 cm, at a lithologic change between Pliocene oozes with sapropels and gray barren clay. Consequently, additional sampling was done in Hole 969B, which proved to be the most complete and least disturbed Miocene/Pliocene boundary sequence at Site 969.

Hole 969B

Hole 969B is located on the Mediterranean Ridge (33°50.399′N, 24°53.065′E, water depth of 2200 m, penetration of 108.3 m). Eleven cores were retrieved with the APC from 0 to 97.9 m. Recovery throughout was close to 100%. The sedimentary sequence recovered in this hole consists of Pliocene–Quaternary nannofossil ooze and nannofossil clay, with more than 80 sapropels from the lower Pliocene through the Holocene. Ten sapropels were observed in Core 160-969B-11H where the Miocene/Pliocene boundary was expected (11H-1, 20–40 cm; 11H-1, 115–120 cm; 11H-2, 40–47 cm; 11H-3, 27–45 cm; 11H-3, 80–97 cm; 11H-5, 0–17 cm; 11H-5, 85–97 cm; 11H-5, 135–150 cm; 11H-6, 50–77 cm; and 11H-6, 120–125 cm). Gray clay was found in Section 160-969B-11H-6, 125 cm, down to the base of Hole 969B (Fig. 3).

Planktonic Foraminifers

Planktonic foraminiferal assemblages are well preserved and scarce to abundant through the early Pliocene sequence. Zone MPl2 is identified in Sample 160-969B-11H-1, 31–33 cm, and 11H-1, 100–102 cm, only. Faunal assemblages include common to abundant *Orbulina universa, Globigerinoides obliquus, G. quadrilobatus, G. sacculifer, G. trilobus, Globorotalia margaritae, Globigerina falconensis, Globigerina bulloides, Globigerinita juvenilis, G. glutinata, Neogloboquadrina acostaensis* dextral, *Zeaglobigerina woodi, Turborotalita quinqueloba, Sphaeroidinellopsis* spp., *Zeaglobigerina decoraperta, Z. nepenthes* group, and rare *Globigerinella obesa, G. siphonifera,* and *Globigerinita uvula.*

Zone MPl1 is identified from Sample 160-969B-11H-2, 30–32 cm, to 11H-6, 124–126 cm. Its thickness is 6.92 m. From Sample 160-969B-11H-2, 30–32 cm, to 11H-3, 130–132 cm, planktonic foraminiferal assemblages are similar to those observed in Hole 967A. The *Sphaeroidinellopsis* acme event is observed from Sample 160-969B-11H-4, 40–42 cm, to 11H-6, 49–50 cm, with the exception of one sample barren of *Sphaeroidinellopsis* (Sample 160-969B-11H-6, 39–40 cm). Its thickness is 3.08 m. Nine sapropels are recorded in the MPl1 biozone. The *Sphaeroidinellopsis* group is also very rare to absent from Sample 160-969B-11H-6, 59–60 to 11H-6, 124–126 cm.

The sediments below Sample 160-969B-11H-6, 124–126 cm consist of gray to dark gray clay. From Sample 160-969B-11H-6, 128–129 cm, downward, the abundances of planktonic foraminifers decreases and the assemblage is dominantly composed of the small-sized (<125 µm) species *T. quinqueloba* together with rarer large-sized specimens of *T. trilobus, G. obliquus, G. bulloides, Z. woodi, N. acostaensis, Sphaeroidinellopsis* spp., and *O. universa* (Table 7).

Although the sediments in this interval contain some marine fauna, they are interpreted to be Messinian "lacustrine deposits" because of the dominant presence of gray clay.

Benthic Foraminifers

Benthic foraminiferal assemblages are very scarce and show very low diversity throughout. Species abundance varies from 0 to 6 specimens per sample (Table 8). In Zones MPl2 and MPl1, benthic assemblages fluctuate in abundance from very rare to rare and include *Siphonina reticulata, G. subglobosa, O. stellatus, C. italicus, G. laevigatus,* and *A. helicinus.* Abundance and species diversity decrease from Sample 160-969B-11H-5, 120–122 cm, downward. The interval where *Sphaeroidinellopsis* spp. are absent or rare is barren of

Table 3. Abundance of size fractions (>151 µm, 40–151 µm, and <40 µm), calcium carbonate content, and stable isotopes of *G. obliquus* and *O. stellatus*, plotted vs. rmcd for Hole 969E.

Core, section, interval (cm)	Depth (rmcd)	$CaCO_3$ (wt%)	Size fraction			Planktonic foraminifers		Benthic foraminifers	
			>151 µm	40–151 µm	<400 µm	$\delta^{13}C$	$\delta^{18}O$	$\delta^{13}C$	$\delta^{18}O$
160-969E									
11H-1, 5-8	117.400	63.000	1.821	3.201	1.341	1.580	–0.149	–0.474	1.311
11H-1, 14-17	117.453	62.000	1.594	3.405	1.280	1.544	–0.158	–0.418	1.405
11H-1, 24-27	117.512	57.000	2.355	4.503	1.632	1.511	–0.169	–0.193	1.459
11H-1, 34-37	117.571	52.000	1.608	3.455	1.282	1.666	–0.473	–0.580	1.309
11H-1, 46-49	117.642	48.000	1.794	3.362	1.471	1.652	–0.336	–0.589	1.255
11H-1, 53-56	117.683	48.000	2.467	4.241	1.602	1.976	–0.399	–0.605	1.263
11H-1, 84-87	117.899	56.000	1.597	3.427	1.486	1.516	–0.555	–0.883	1.639
11H-1, 95-97	117.983	56.000	2.600	4.369	3.079	1.482	–0.609	–0.916	1.609
11H-1, 104-107	118.060	56.000	2.477	4.360	1.361	1.619	–0.578	–0.735	1.368
11H-1, 115-117	118.144	63.000	3.212	4.832	1.664	1.588	–0.392	–0.754	1.488
11H-2, 5-8	118.470	66.000	3.333	4.386	1.678	1.480	–0.204	–0.533	1.393
11H-2, 14-17	118.552	62.000	3.130	4.319	1.634	1.465	–0.434	–0.418	1.485
11H-2, 24-27	118.662	63.000	3.661	4.213	1.523	1.677	–0.505	–0.538	1.554
11H-2, 34-37	118.772	60.000	4.163	4.843	1.748	1.451	–0.135	–0.633	1.474
11H-2, 44-47	118.881	64.000	4.225	5.883	2.004	1.340	–1.280	–0.947	1.444
11H-2, 53-56	118.980	67.000	5.840	8.155	3.183	1.579	–0.741	–0.930	1.600
11H-2, 64-66	119.095	68.000	6.080	7.242	3.272	1.461	–0.846	–0.881	1.574
11H-2, 74-76	119.204	60.000	2.618	3.320	1.176	1.710	–0.432	–0.480	1.567
11H-2, 87-89	119.331	68.000	2.710	3.950	1.520	1.578	–0.299	–0.498	1.456
11H-2, 104-107	119.501	66.000	5.617	4.782	2.088	1.341	–0.464	–0.689	1.415
11H-2, 114-116	119.594	66.000	6.598	5.007	1.994	0.626	–1.881	–0.587	1.484
11H-2, 124-127	119.696	68.000	7.431	5.953	2.370	0.736	–2.295	–0.776	1.503
11H-2, 134-136	119.789	70.000	6.350	6.932	2.823	0.357	–2.431	–0.844	1.505
11H-2, 144-147	119.891	68.000	5.806	6.652	2.976	1.252	–0.394	–1.088	1.555
11H-3, 5-8	119.998	77.000	7.262	8.059	3.385	1.257	–0.205	–1.215	1.407
11H-3, 14-17	120.086	78.000	6.043	6.970	2.325	1.384	–0.310	–1.022	1.503
11H-3, 24-26	120.174	67.000	2.484	3.461	1.045	1.628	–0.195	–0.401	1.729
11H-3, 34-37	120.281	70.000	1.960	3.320	1.106	1.633	–0.295	–0.393	1.671
11H-3, 44-47	120.379	80.000	2.800	4.060	1.250	1.665	–0.337	–0.613	1.617
11H-3, 57-60	120.505	76.000	2.810	4.557	1.531	1.753	–0.426	–0.523	1.538
11H-3, 64-66	120.569	60.000	1.926	2.830	1.242	1.014	0.061	–0.966	1.700
11H-3, 73-76	120.661	66.000	2.091	2.901	1.204	1.111	0.323	–0.831	1.777
11H-3, 87-89	126.087	64.000	1.491	2.446	0.585	1.325	–0.083	–0.790	1.916
11H-3, 97-100	126.156	56.000	1.562	2.649	1.096	1.093	0.254	–0.677	1.627
11H-3, 104-107	126.202	55.000	1.773	2.900	0.978	1.127	–0.011	–0.737	1.413
11H-3, 114-116	126.265	51.000	1.858	2.590	0.985	1.181	–0.015	–0.623	1.702
11H-3, 124-127	126.334	56.000	1.484	2.695	0.944	1.295	–0.137	–0.946	1.486
11H-3, 134-136	126.396	64.000	0.765	1.410	0.758	1.405	0.100	–0.896	1.541
11H-3, 144-147	126.465	64.000	0.037	0.130	1.184	1.459	–0.522	–0.847	1.228
11H-4, 17-20	126.626	60.000	2.987	4.700	1.829	1.134	–0.565	–0.699	1.297
11H-4, 34-37	126.760	67.000	0.931	2.409	0.886	1.133	–0.221	–0.651	1.250
11H-4, 44-47	126.840	62.000	2.584	3.230	1.233	1.299	–0.036	–0.617	0.980
11H-4, 57-60	126.943	60.000	1.765	3.174	1.164	1.137	–0.234	–0.635	1.279
11H-4, 64-66	126.994	62.000	3.117	3.750	1.292	0.973	–0.297	–0.709	1.267
11H-4, 74-77	127.078	64.000	2.902	2.909	1.219	1.249	–0.142	–0.888	1.175
11H-4, 84-87	127.157	60.000	3.517	3.771	1.421	1.085	–0.185	–0.604	1.277
11H-4, 94-97	127.236	66.000	4.826	6.542	2.923	1.124	–0.677	—	—
11H-4, 102-104	127.296	72.000	4.640	6.224	1.896	1.394	–0.033	–1.110	0.924
11H-4, 114-116	127.391	66.000	3.177	3.319	1.214	1.281	–0.031	–0.702	1.412
11H-4, 124-127	127.474	64.000	3.349	3.285	1.133	1.202	–0.005	–0.472	1.462
11H-4, 137-139	127.565	64.000	3.131	3.640	1.267	1.227	0.095	–0.840	1.400
11H-4, 144-147	127.633	61.000	2.611	3.443	1.072	1.222	–0.013	–0.842	1.041
11H-5, 4-7	127.712	60.000	2.716	3.452	1.129	1.279	–0.189	–0.600	1.211
11H-5, 14-17	127.791	63.000	2.529	3.295	0.337	1.489	–0.465	–0.893	0.876
11H-5, 44-47	128.007	74.000	2.379	3.917	2.123	1.423	–0.114	–0.858	0.970
11H-5, 54-57	128.062	78.000	4.087	5.380	1.785	1.391	–0.230	–0.939	1.078
11H-5, 64-66	128.115	77.000	3.202	4.061	1.306	1.394	–0.247	–0.797	1.187
11H-5, 74-77	128.173	70.000	4.971	4.513	1.887	1.496	0.077	–0.788	1.109
11H-5, 84-87	128.229	66.000	3.008	3.018	1.282	1.485	–0.099	–0.828	0.954
11H-5, 94-97	128.285	62.000	2.819	2.552	1.239	1.331	–0.108	–0.861	1.246
11H-5, 104-106	128.337	60.000	1.438	2.013	1.105	1.260	–0.216	–0.931	1.190
11H-5, 111-113	128.376	66.000	1.377	1.797	0.981	1.669	–0.636	–0.591	1.187
11H-5, 134-137	128.553	70.000	3.666	4.293	1.344	1.609	–0.663	–0.732	0.885
11H-5, 144-147	128.657	64.000	2.811	3.054	1.199	1.491	–0.481	—	—
11H-6, 4-7	128.762	66.000	2.218	3.373	1.046	1.348	–0.541	–1.068	1.550
11H-6, 14-17	128.866	87.000	1.343	2.527	1.319	—	—	—	—
11H-6, 24-27	130.683	18.000	0.011	0.011	0.036	—	—	—	—
11H-6, 34-37	130.875	14.000	0.008	0.023	0.039	—	—	—	—
11H-6, 44-47	131.067	14.000	0.008	0.015	0.031	—	—	—	—
11H-6, 48-51	131.135	14.000	0.006	0.013	0.032	—	—	—	—
11H-6, 54-57	131.200	16.000	0.013	0.013	0.039	—	—	—	—
11H-6, 74-77	131.400	14.000	0.010	0.029	0.048	—	—	—	—
11H-6, 84-87	131.500	12.000	0.006	0.026	0.040	—	—	—	—
11H-6, 94-97	131.600	13.000	0.015	0.015	0.039	—	—	—	—
11H-6, 105-108	131.710	14.000	0.032	0.032	0.024	—	—	—	—
11H-6, 113-116	131.790	13.000	0.007	0.020	0.039	—	—	—	—
11H-6, 124-127	131.900	16.000	0.005	0.021	0.032	—	—	—	—
11H-6, 134-137	132.000	16.000	0.008	0.015	0.038	—	—	—	—
11H-6, 143-145	132.085	14.000	0.000	0.008	0.044	—	—	—	—

Table 4. Distribution and abundance of Pliocene planktonic foraminifers in Hole 967A.

Subseries	Pl. Foram. Zones	160-967A Core, section, interval (cm)	*O. universa*	*G. obesa*	*G. quadrilobatus*	*G. obliquus*	*G. sacculifer*	*G. falconensis*	*G. trilobus*	*Sphaeroidinellopsis* group	*N. dutertrei*	*G. bulloides*	*N. acostaensis* sinistral	*G. siphonifera*	*G. ruber*	*Z. nepenthes* group	*B. digitata*	*N. acostaensis* dextral	*Z. woodi*	*G. scitula*	*T. juvenilis*	*T. glutinata*	*N. pachyderma* dextral	*T. quinqueloba*	*G. gomitulus*	*T. uvula*	*Z. decoraperta*	*Z. nepenthes*	*G. margariate*	*S. seminulina*	*S. subdehiscens*	*S. kochi*	*N. pachyderma* sinistral	*S. globigerum*	*T. anfracta*	*"G. "venezuelana*	*G. bulbosa*	*G. menardiigroup*	*S. dehiscens*	Species abundance	Total specimens
early Pliocene		12CC-42-44	25	5	9	59	19	84	19	-	?	7	x	x	2	8	x	8	12	x	17	28	x	5	2	4	2	1	10	-	-	-	-	-	-	-	-	-	-	27	326
		13H-1, 27-29	23	8	3	49	2	66	12	4	-	4	2	x	-	14	-	10	8	6	17	24	-	3	-	2	1	-	49	x	x	x	-	-	-	-	-	-	-	24	307
		13H-1, 35-37	27	5	-	75	1	114	1	2	x	3	-	-	4	19	-	2	18	1	10	27	-	x	-	2	8	2	2	x	-	x	-	-	-	-	-	-	-	23	323
	MPl2	13H-1, 77-79	40	3	10	62	4	85	12	12	-	4	1	-	3	23	-	5	2	x	17	10	-	x	x	1	2	-	4	-	x	x	-	-	x	-	-	-	-	25	300
		13H-1, 107-109	23	4	12	42	8	33	31	-	-	-	4	2	3	22	-	50	1	1	19	23	-	x	-	x	-	2	26	-	-	-	-	-	-	-	-	4	-	-	21	310
		13H-1, 117-119	19	5	4	69	7	60	19	10	-	-	1	x	-	28	-	10	4	-	25	35	-	x	1	1	5	1	11	x	x	x	-	-	-	-	-	-	-	23	315
		13H-2, 19-21	21	3	13	55	8	42	15	-	-	-	2	4	-	22	-	23	4	1	34	22	-	x	-	5	8	3	20	-	-	-	-	-	-	-	-	1	x	22	306
		13H-2, 35-37	19	1	25	56	11	29	36	-	-	1	-	1	-	26	-	42	4	x	17	19	x	3	-	2	6	2	-	x	-	x	-	-	-	-	3	4	-	24	307
	MPl1	13H-2, 67-69	70	1	-	66	1	77	8	-	-	-	1	-	-	18	-	6	5	x	16	28	x	2	-	x	6	2	-	-	-	-	-	-	-	-	x	-	-	19	307
		13H-2, 94-96	43	7	9	61	5	48	4	-	-	9	-	1	1	36	-	8	11	1	20	28	-	1	-	1	5	8	?	-	-	-	-	-	x	-	-	-	-	23	307
		13H-2, 106-108	13	4	19	52	12	15	38	-	-	6	x	2	1	12	-	89	1	x	17	16	x	x	1	x	1	2	-	-	-	-	-	-	-	-	-	-	-	23	301
		13H-3, 25-27	53	2	-	47	-	54	3	71	-	2	-	x	-	23	-	3	6	x	20	10	-	1	-	x	6	6	-	x	x	x	-	x	-	-	-	-	-	21	307
		13H-3, 33-35	34	3	14	70	6	9	14	74	-	2	-	2	3	6	-	15	4	x	29	11	-	2	1	1	4	2	-	x	x	x	-	-	-	-	-	-	-	24	306
	Spha	13H-3, 69-71	38	7	3	38	1	5	8	78	-	2	3	4	3	30	-	19	11	2	21	14	-	1	-	2	10	4	-	x	x	x	x	-	-	-	-	-	-	26	304
		13H-3, 105-107	56	13	12	49	4	4	8	73	-	4	-	6	-	12	-	12	5	4	23	9	x	x	-	3	6	4	-	x	x	x	-	-	-	-	-	-	-	23	307
		13H-3, 113-115	56	2	6	61	-	16	3	87	-	1	-	2	1	21	-	4	5	-	26	23	-	x	-	x	5	2	-	x	x	x	-	-	-	-	-	-	-	22	321

Note: x = simple occurrence, but not represented in the 300 specimens counted.

Table 5. Distribution of planktonic foraminifers in Messinian and early Pliocene (Zanclean) sediments.

Subseries (Stage)	Pl. Foram. Zones	160-967A Core, section, interval (cm)	Barren Samples	Terrigenous	Pliocene forms	Dwarf forms	*C. pannonica*	*Ammonia* sp.	*Elphidium* sp.	Paratethian Ostracods	*P. pseudoscitulus*	*Globigerinatheka* sp.	*Acarinina* sp.	*A. soldadoensis*	*T. griffinae*	*A. pentacamerata*	*A. bulbrooki*	*Z. ampliapertura*	*D. galavisi*	*S. angiporoides*	*S. utilisindex*	*Pseudohastigerina* sp.	*C. cubensis*	*P. opima*	*P. pseudokugleri*	*P. kugleri*	*"G." ciperoensis* group	*C. chipolensis*	*G. dehiscens*	*P. acrostoma*	*P. transitoria*
early Pliocene (Zancl.)	MPl1	13H-4, 25-27	-	a	r	-	-	-	-	-	-	-	-	-	-	-	-	-	-	-	x	x	-	x	-	-	-	-	-	-	-
		13H-4, 43-45	-	a	x	-	-	-	-	-	-	-	-	-	-	-	-	-	-	-	-	x	x	-	x	-	-	-	-	-	-
		13H-4, 78-80	-	-	-	x	-	-	-	-	-	-	-	-	-	-	-	-	-	-	-	x	-	-	-	-	-	-	-	-	-
		13H-4, 109-111	-	-	x	-	x	-	x	x	-	-	-	-	-	-	-	-	-	-	-	-	-	-	-	-	-	-	-	-	-
late Miocene (Messin.)	Not zoned	13H-5, 13-15	-	-	-	x	frg	x	-	-	-	-	-	-	-	-	-	-	-	-	-	-	-	-	-	-	-	-	-	-	-
		13H-5, 79-81	-	-	x	x	-	x	-	-	-	-	-	-	-	-	-	-	-	-	-	-	-	-	-	-	-	-	-	-	-
		13H-5, 103-105	-	-	x	x	x	x	-	-	-	-	-	-	-	-	-	-	-	-	-	-	-	-	-	-	-	-	-	-	-
		13H-6, 24-26	-	a	x	-	r	r	-	-	-	-	-	-	-	-	-	-	-	-	-	x	x	-	x	-	-	-	-	-	-
		13H-6, 37-39	-	a	a	-	-	-	-	-	-	-	-	-	-	-	-	-	-	-	-	-	-	-	-	-	-	-	-	-	-
		13H-6, 79-81	-	-	c	-	-	-	-	-	-	-	-	-	-	-	-	-	-	-	-	-	-	-	-	-	-	-	-	-	-
		13H-6, 117-119	-	r	a	-	x	-	-	-	-	-	-	-	-	-	-	-	-	-	-	-	-	-	-	-	-	-	-	-	-
		13H-7, 12-14	-	-	x	-	a	x	-	-	-	-	x	-	-	-	-	-	-	-	x	-	x	-	-	x	x	-	-	-	-
		13H-7, 29-31	-	-	x	-	x	x	-	-	-	-	-	x	x	x	x	-	-	-	-	-	-	-	-	-	-	-	-	-	-
		14X-1, 50-52	-	-	vr	-	c	x	-	-	-	-	-	-	-	-	-	-	-	-	-	-	-	-	-	-	-	-	-	-	-
		14X-1, 101-103	-	-	x	-	-	-	-	-	-	-	-	-	-	-	-	x	x	x	x	-	x	-	-	-	-	x	x	x	-
		14X-2, 21-23	-	-	r	-	c	a	-	-	-		-	-	-	-	-	x	-	-	-	-	-	-	-	-	-	-	-	-	x
		14X-2, 114-116	-	-	-	-	x	x	-	-	x	x	x	-	-	-	-	x	-	-	-	-	-	-	-	-	x	x	-	-	x
		14X-3, 40-42	-	-	-	-	x	r	-	-	x	-	-	-	-	-	-	-	-	-	-	-	-	-	-	-	-	-	-	-	-
		14X-3, 124-126	b	-	-	-	-	-	-	-	-	-	-	-	-	-	-	-	-	-	-	-	-	-	-	-	-	-	-	-	-
		14X-4, 14-16	-	-	vr	-	x	r	-	-	-	-	-	-	-	-	-	-	-	-	-	-	-	-	-	-	-	-	-	-	-
		14X-4, 120-123	-	-	x	-	-	-	-	-	-	x	-	-	-	-	x	-	-	-	-	-	-	-	-	-	-	-	-	-	-
		14X-5, 19-21	-	-	vr	-	-	-	-	-	-	x	-	-	-	-	-	-	-	-	-	-	-	-	-	-	-	-	-	-	-
		14X-5, 97-100	b	-	-	-	-	-	-	-	-	-	-	-	-	-	-	-	-	-	-	-	-	-	-	-	-	-	-	-	-
		15X-1, 73-75	-	-	r	-	-	-	-	-	-	-	x	-	-	-	-	-	-	-	x	-	-	-	x	-	-	-	-	x	-
		15X-1, 131-133	-	-	-	-	x	-	x	-	-	x	-	-	x	-	-	x	-	-	-	-	x	-	-	-	x	-	-	x	-
		15X-2, 34-35	b	-	-	-	-	-	-	-	-	-	-	-	-	-	-	-	-	-	-	-	-	-	-	-	-	-	-	-	-
		15X-2, 129-131	-	-	-	-	-	-	-	-	-	-	-	-	-	-	-	-	-	-	x	-	-	-	x	-	x	-	x	x	-
		15X-3, 24-31	-	-	r	-	-	-	-	-	-	x	x	-	-	-	-	-	-	x	-	-	-	-	-	-	x	x	x	x	-
		15X-3, 75-77	-	-	-	-	-	-	-	-	-	x	-	-	-	x	x	-	-	-	-	-	-	-	-	-	-	-	x	-	-
		15X-4, 6-8	-	-	r	x	x	x	-	-	-	-	-	-	-	-	-	-	-	-	-	-	-	-	-	-	-	-	-	x	-
		15X-CC, 15-17	-	-	-	-	-	-	-	-	-	x	-	-	-	x	-	-	-	-	x	-	-	-	-	-	-	-	-	x	-
		16X-1, 84-86	-	-	-	-	-	-	-	-	-	x	-	-	-	-	x	-	x	-	-	x	x	-	-	-	-	x	-	-	-

Note: vr = very rare, r = rare, c = common, a = abundant, d = dominant, frg = fragments.

benthic foraminifers (Sample 160-969B-11H-6, 59–60 cm, to 11H-6, 124–126 cm).

Hole 969E

Hole 969E is located on the Mediterranean Ridge (33°50.462′N, 24°52.98′E, water depth of 2201.1, penetration of 97.9 m). Eleven cores were retrieved with the APC from 0 to 97.9 m. Recovery throughout was close to 100%. Coring was terminated when the sedimentary sequence became extremely firm while drilling for Core 160-969E-12H. The sedimentary sequence recovered in this hole is very similar to that recovered at Hole 969B.

Six sapropels were observed in Core 160-969E-11H where the Miocene/Pliocene boundary was expected (11H-1, 67–77 cm; 11H-3, 137 to 11H-4, 10 cm; 11H-4, 25–27 cm; 11H-5, 25–40 cm; 11H-5, 127–130 cm; and 11H-6, 15–20 cm). Gray clay was encountered at the top of Section 160-969E-11H-6, 23 cm, down to the end of the hole. Shore-based studies revealed that several faults are present in

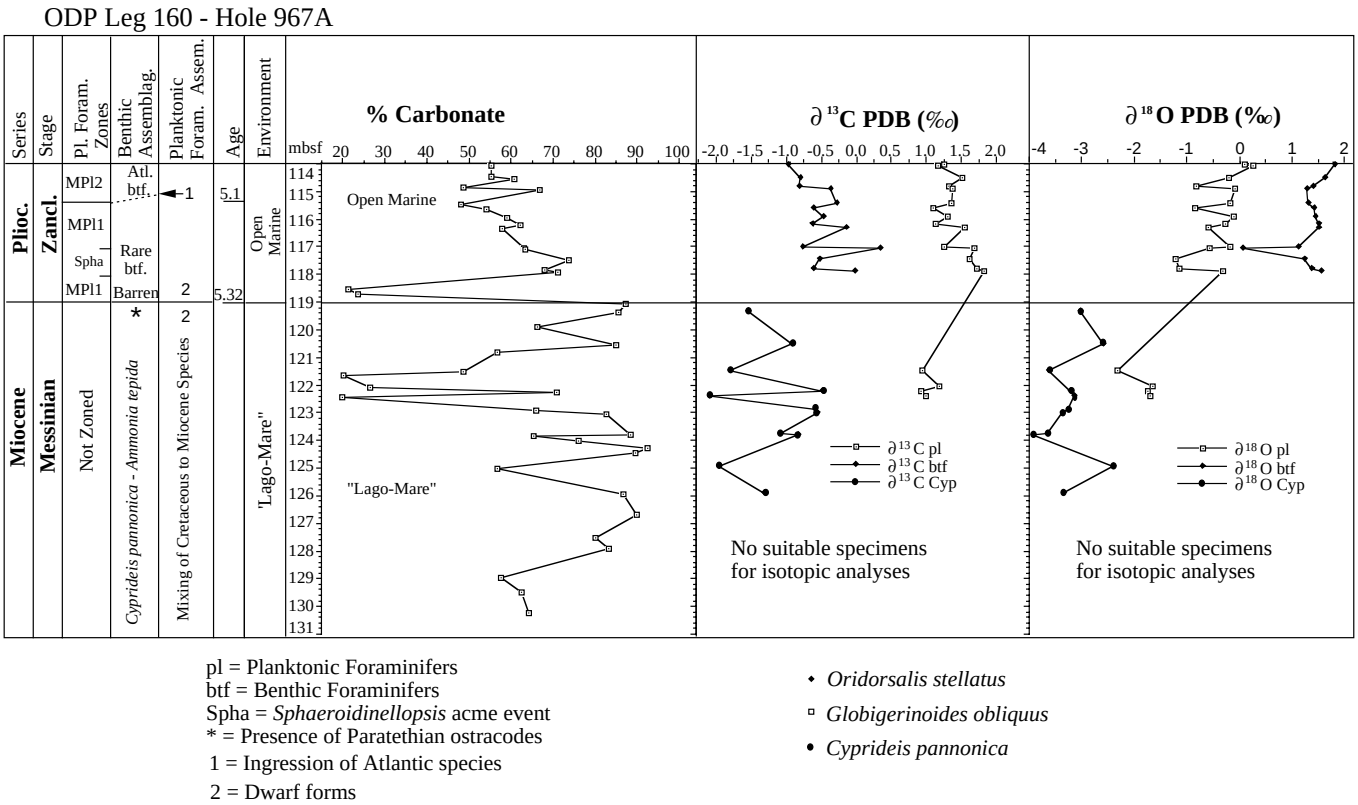

Figure 4. Summary of chemo- and biostratigraphy of the uppermost Miocene and lowermost Pliocene sediments of Hole 967A. Numerical age from Berggren et al. (1995).

this hole. The most important ones occur within Section 11H-3 and at the contact between the calcareous oozes and the gray clay (Sakamoto et al., Chap. 4, this volume; T. Sakamoto, pers. comm., 1997).

Planktonic Foraminifers

Because a fault was present, Zone MPl1 is missing at Hole 969E. Core 160-969E-11H contains sediments attributed to Zone MPl2. Planktonic foraminiferal assemblages are well preserved and rich throughout. They consist of the typical lower Pliocene fauna previously described for Holes 967A and 969B. No range charts were produced for this hole, since the lowermost part of the Pliocene succession is missing.

Benthic Foraminifers

Benthic foraminifers assemblages from this hole are abundant and rich and include all the species observed for Hole 967A (Table 6).

GEOCHEMICAL RESULTS

Calcium Carbonate

The calcium carbonate content varies from 19% to more than 80% of the pelagic oozes in Hole 967A, where the larger amplitude fluctuations are observed. In particular, low calcium carbonate content peaks are observed for Samples 160-967A-13H-4, 25–27 cm and 13H-4, 43–45 cm (21.31% and 23.75%) and for Samples 160-967A-13H-6, 37–39 cm, 13H-6, 79–81 cm, and 13H-6, 117–119 cm (20.25%, 26.49% and 29.78%, respectively; Table 1, Fig. 4). A sharp drop in carbonate content from about 51% to 13% and from 87% to 18% (Samples 160-969B-11H-6, 128–129 cm, and 160-969E-11H-6, 24–27 cm, respectively) is observed in both Holes 969B and 969E in correspondence to the change in lithology (Tables 1–3; Figs. 4–6).

Stable Isotopes

The stable isotope stratigraphy for Holes 967A, 969B, and 969E are shown in Figures 4–6, respectively. In Hole 967A, the earliest Pliocene $\delta^{18}O$ values for both planktonic and benthic foraminifers tend to show an upward enrichment in ^{18}O, whereas the $\delta^{13}C$ values tend toward a depletion in ^{13}C (Fig. 4). Fluctuations in the $\delta^{18}O$ appear to be related to the fluctuations in abundance of the warm water *Globigerinoides* group (Fig. 7). There is a notable negative reversal in the $\delta^{13}C$ values of the benthic foraminifers at the top of the *Sphaeroidinellopsis* acme event. A similar reversal was observed in a high-resolution study of the earliest Pliocene sediments deposited at ODP Leg 107, Site 652 in the Tyrrhenian Sea (McKenzie et al., 1990). The ostracode *C. pannonica* displays stable isotope values markedly more negative than those observed for either the benthic or planktonic foraminifers (Fig. 4; Table 1).

In Hole 969B, the $\delta^{13}C$ values appear to be rather invariant for planktonic foraminifers (Fig. 5), whereas fluctuations observed in $\delta^{18}O$ appear to correspond to fluctuations in the abundance of the warm water *Globigerinoides* group (Fig. 8). Benthic foraminifers show two major positive shifts in their $\delta^{13}C$ values in the middle-upper part of the *Sphaeroidinellopsis* acme event. The uppermost shift coincides with a corresponding but negative excursion in the benthic $\delta^{18}O$ value. A similar trend was also observed in the Hole 967A sequence and the Tyrrhenian Sea (McKenzie et al., 1990).

In the case of Hole 969E, the isotope stratigraphy tends to be rather monotonous but typical for a marine system. In the upper part of

Table 6. Distribution and species abundance of Pliocene benthic foraminifers in Hole 967A.

Subseries	Pl. Foram. Zones	160-967A Core, section, interval (cm)	*G. laevigatus*	*V. marmorea*	*O. stellatus*	*G. subglobosa*	*P. quadriloba*	*Q. laevigata*	*P. alternans*	*K. bradyi*	*C. pachyderma*	*B. punctata*	*U. peregrina*	*P. ariminensis*	*P. quinqueloba*	*C. italicus*	*C. ungerianus*	*U. pygmaea*	*S. antillea*	*B. nodosaria*	*S. monilis*	*A. helicinus*	*U. rutila*	*E. pusillus*	*L. lobatula*	*S. schlumbegeri*	*B. dilatata*	*P. robertsonianus*	*S. reticulata*	*G. soldanii*	*D. leguminiformis*	*L. inornata*	*P. bulloides*	*E. bradyi*	*O. faveolata*	*P. salisbury*	*P. exigua*	*P. bradyi*	*L. gibba*	*A. stelligerum*	*L. rotulata*	*C. serpens*	Species abundance
early Pliocene	MPl2	12CC-42-44	x	-	x	x	x	-	x	x	-	-	-	-	-	x	x	x	x	-	-	-	-	-	x	-	-	x	x	x	-	-	-	-	-	-	-	x	x	x	-	-	23
		13H-1, 27-29	x	x	x	x	x	-	x	x	x	x	-	x	x	x	-	-	-	x	x	x	-	-	-	-	-	-	x	-	x	x	x	-	-	-	-	x	x	-	-	-	25
		13H-1, 35-37	x	x	x	-	-	-	-	-	-	x	-	-	-	x	-	-	-	-	-	-	-	-	-	-	-	-	x	x	-	-	-	x	-	-	-	-	-	-	-	-	9
		13H-1, 77-79	-	x	x	-	-	-	-	-	-	x	-	x	-	x	x	x	x	x	x	x	-	-	-	x	-	-	x	x	x	x	x	-	-	-	-	-	-	-	-	-	20
		13H-1, 107-109	x	x	x	-	-	-	x	x	-	x	-	x	-	x	x	x	x	-	x	-	x	-	x	-	x	x	x	x	x	-	-	-	-	-	-	x	x	x	-	-	32
		13H-1, 117-119	x	x	x	-	-	-	-	x	x	x	-	x	-	x	x	-	-	-	-	x	-	-	-	-	-	-	x	x	x	-	-	-	-	-	-	-	-	-	x	-	20
		13H-2, 19-21	x	x	x	x	-	-	x	-	-	-	-	x	-	x	x	-	x	x	x	x	-	-	-	x	-	x	x	x	x	x	-	x	x	-	-	-	x	-	x	24
		13H-2, 35-37	x	x	x	x	-	-	x	x	-	x	-	x	-	x	-	-	x	x	-	-	x	-	-	x	-	-	x	x	-	-	-	-	-	-	-	x	-	-	-	-	20
	MPl1	13H-2, 67-69	x	-	x	x	-	-	-	x	cf	-	x	x	-	x	x	-	-	x	-	x	-	-	x	x	-	-	x	x	x	-	-	x	-	-	-	-	x	-	x	-	21
		13H-2, 94-96	x	-	x	x	-	x	x	-	x	-	x	-	-	x	x	-	x	-	-	x	-	-	-	-	-	-	x	x	x	x	-	x	x	-	-	-	vr	x	x	x	22
		13H-2, 106-108	x	-	x	x	x	-	x	x	-	-	x	x	-	x	x	x	x	x	-	-	-	x	-	x	-	vr	x	x	x	x	x	x	x	x	-	-	-	-	-	26
		13H-3, 25-27	x	x	x	x	-	x	-	x	-	-	-	-	-	-	x	x	-	-	-	x	x	-	x	x	x	-	-	-	-	-	-	-	-	-	-	-	-	-	-	-	13
		13H-3, 33-35	x	x	x	x	-	x	x	x	-	-	x	-	x	x	x	x	x	x	x	x	x	x	-	-	-	-	-	-	-	-	-	-	-	-	-	-	-	-	-	-	18
	Spha	13H-3, 69-71	x	x	x	x	-	x	-	-	-	-	x	x	x	-	-	-	-	-	-	-	-	-	-	-	-	-	-	-	-	-	-	-	-	-	-	-	-	-	-	-	8
		13H-3, 105-107	x	-	x	x	-	x	x	x	x	x	x	-	-	-	-	-	-	-	-	-	-	-	-	-	-	-	-	-	-	-	-	-	-	-	-	-	-	-	-	-	9
		13H-3, 113-115	x	x	x	c	x	x	-	-	-	-	-	-	-	-	-	-	-	-	-	-	-	-	-	-	-	-	-	-	-	-	-	-	-	-	-	-	-	-	-	-	6

Note: vr = very rare.

Table 6 (continued).

Subseries	Pl. Foram. Zones	160-967A Core, section, interval (cm)	*S. tenuis*	*M. perparva*	*L. clavata*	*V. carinata*	*B. subspinescens*	*V. pennatula*	*L. cultrata*	*M. communis*	*S. planoconvexa*	*C. ornatus*	*P. ostoensis*	*S. hispida*	*Marginulina* sp.	*V. sulcata*	*Q. bicarinata*	*Q. viennensis*	*S. bulloides*	*C. rudis*	Speciesabundance
early Pliocene	MPl2	12CC-42-44	-	-	-	-	-	-	x	x	-	x	x	-	-	-	-	-	-	x	23
		13H-1, 27-29	-	-	-	-	-	x	-	x	-	-	x	-	-	-	-	-	-	-	25
		13H-1, 35-37	-	-	-	-	-	-	x	-	-	-	-	-	-	-	-	-	-	-	9
		13H-1, 77-79	-	-	x	-	-	x	-	-	-	-	-	-	-	-	-	-	-	-	20
		13H-1, 107-109	-	-	-	-	x	-	x	-	-	x	x	x	x	?	x	x	x	-	32
	MPl1	13H-1, 117-119	x	-	-	-	-	x	x	x	x	-	-	-	-	-	-	-	-	-	20
		13H-2, 19-21	-	-	-	-	-	x	-	-	-		-	-	-	-	-	-	-	-	24
		13H-2, 35-37	-	-	x	cf	x	-	-	-	-	-	-	-	-	-	-	-	-	-	20
		13H-2, 67-69	x	x	-	-	-	-	-	-	-	-	-	-	-	-	-	-	-	-	21
		13H-2, 94-96	-	-	-	-	-	-	-	-	-	-	-	-	-	-	-	-	-	-	22
		13H-2, 106-108	-	-	-	-	-	-	-	-	-	-	-	-	-	-	-	-	-	-	26
		13H-3, 25-27	-	-	-	-	-	-	-	-	-	-	-	-	-	-	-	-	-	-	13
		13H-3, 33-35	-	-	-	-	-	-	-	-	-	-	-	-	-	-	-	-	-	-	18
	Spha	13H-3, 69-71	-	-	-	-	-	-	-	-	-	-	-	-	-	-	-	-	-	-	8
		13H-3, 105-107	-	-	-	-	-	-	-	-	-	-	-	-	-	-	-	-	-	-	9
		13H-3, 113-115	-	-	-	-	-	-	-	-	-	-	-	-	-	-	-	-	-	-	6

the MPl2 Biozone, there is, however, an excursion toward significantly more negative $\delta^{18}O$ values (Fig. 6).

The stable isotope signals of the planktonic foraminifers that occur associated with brackish water ostracodes in Hole 967A are slightly more enriched in the heavier isotopes relative to the ostracodes but are depleted relative to the values for the foraminifers from the overlying marine sequence (Table 1; Fig. 4).

DISCUSSION

At Hole 967A, located on the base of the northern slope of the Eratosthenes Seamount, the identification of the Miocene/Pliocene boundary coincides with the lower boundary of the lithostratigraphic Unit II and is located between 119.1 and 119.4 mbsf (between Samples 160-967A-13H4, 78–80 cm, and 13H-4, 109–111 cm; Emeis, Robertson, Richter, et al., 1996). At the same depth, a shift from a high content of inorganic and non-marine calcite to a high content of a biogenic calcite typical of the marine pelagic ooze is also observed (Emeis, Robertson, Richter, et al., 1996). The presence of the well-preserved ostracodes with closed valves in Sample 160-967A-13H-4, 109–111 cm, supports this placement of the Miocene/Pliocene boundary, as it represents the uppermost occurrence of these brackish water species.

At Site 969, some 700 km to the west of the previous location, on the inner plateau of the Mediterranean Ridge south of Crete, the identification of the Miocene/Pliocene boundary coincides with a marked lithologic change, which is recorded in three discrete holes (Holes 969A, 969B, 969E), as shown in Figure 9. The overlying unit is represented by early Zanclean nannofossil-foraminiferal oozes with intercalated sapropels, whereas the underlying unit is gray mud, with rarer and generally dwarf microfossils consisting of dominant *T. quinqueloba*. The biostratigraphic correlation shown in Figure 9 demonstrates that the sapropels recorded in Section 160-969E-11H-6 are not correlatable with most of sapropels of Core 160-969B-11H, but are younger. A sediment thickness of some 6 m is missing in Hole 969E. The sedimentary sequences record an unstable tectonic setting during their deposition and immediately afterward. Unfortunately, the penetration was interrupted, and no older Messinian lithologies were reached.

At Hole 969B the Miocene/Pliocene boundary is located between 97.1 and 97.2 mbsf (between Samples 160-969B-11H-6, 124–126 cm, and 11H-6, 128–129 cm). The pre-Pliocene sediments recovered on the Mediterranean Ridge are fine grained and similar to those recovered in deep-sea settings at DSDP Site 374 on the Messina abyssal plain in the Ionian Basin (Hsü, Montadert, et al., 1978) and Aphrodite Crater on the Western Mediterranean Ridge (Blechschmidt et al., 1982).

The presence of planktonic foraminifers associated with brackish water ostracodes in Hole 967A and with the gray clay in Hole 969B below the interpreted Miocene/Pliocene boundary deserves comment. In fact, the stable isotope composition of *C. pannonica* indicates that this crustacean lived in a Lago Mare environment characterized by brackish water, distinctly different form the marine envi-

Table 7. Distribution and abundance of Pliocene and upper Messinian planktonic foraminifers in Hole 969B.

Subseries	Pl. Foram. Zones	160-969B Core, section, interval (cm)	*G. trilobus*	*G. obliquus*	*G. bulloides*	*G. scitula*	*Z. woodi*	*G. juvenilis*	*N. acostaensis* dextral	*G. glutinata*	*Z. decoraperta*	*G. falconensis*	*Z. nepenthes* group	*Sphaeroidinellopsis* group	*O. universa*	*G. quadrilobatus*	*G. sacculifer*	*N. acostaensis* sinistral	*T. quinqueloba*	*Z. rubescens*	*G. obesa*	*G. siphonifera*	*G. uvula*	*Z. nepenthes*	*G. bulbosa*	*G. ruber*	*G. gomitulus*	*N. pachyderma* sinistral	*G. elongatus*	*N. pachyderma* dextral	*B. digitata*	*T. anfracta*	*H. pelagica*	*G. margaritae*	Species abundance	Total specimens
early Pliocene		11H-1, 31-33	-	3	-	-	3	3	1	-	1	4	1	-	1	-	-	-	x	-	-	-	-	-	-	-	-	-	-	-	-	-	-	9	17
	MPl2	11H-1, 100-102	7	69	6	-	10	22	33	28	15	63	19	-	10	5	4	-	4	-	1	1	2	1	1	-	-	-	-	-	-	-	5	20	306
		11H-2, 30-32	1	60	1	1	9	28	33	27	9	91	5	-	42	-	1	2	7	-	x	-	x	-	-	-	-	-	-	-	-	-	-	18	317
	MPl1	11H-2, 100-102	2	21	-	x	27	27	91	39	11	41	16	1	22	1	-	-	5	-	-	-	x	-	5	-	-	-	-	-	-	-	1	17	310
		11H-3, 40-42	34	7	1	-	7	24	16	9	1	15	9	2	9	3	3	1	x	-	-	-	-	-	-	-	-	-	-	-	-	-	-	16	141
		11H-3, 130-132	2	66	2	x	17	18	16	23	4	111	13	3	18	3	-	1	x	-	-	-	x	3	-	-	-	-	-	-	-	-	-	19	300
		11H-4, 40-42	8	66	5	x	10	10	32	17	15	52	6	19	36	16	4	2	6	-	-	-	-	1	-	-	-	-	-	-	-	-	-	20	305
		11H-4, 120-122	5	48	4	3	14	17	18	10	3	109	12	35	42	x	1	1	1	-	x	-	-	-	-	-	-	-	-	-	-	-	1	20	324
		11H-5, 3-5'	41	17	2	9	3	25	66	24	4	14	5	23	36	19	12	-	1	1	2	2	-	-	-	-	-	-	-	-	-	1	-	22	307
		11H-5, 7-9'	23	54	-	x	13	16	6	6	3	15	4	57	67	34	2	1	x	-	-	-	-	-	-	-	-	-	-	-	-	-	-	18	301
	Sphaeroidinellopsis acme	11H-5, 30-32	3	65	-	1	16	14	20	8	12	74	2	28	47	4	3	1	2	-	-	1	-	1	-	-	-	-	-	-	x	-	-	21	302
		11H-5, 50-52	9	35	6	2	7	13	43	26	3	45	9	33	47	12	6	3	1	-	3	-	3	-	-	-	-	-	-	-	-	-	-	21	306
		11H-5, 70-72	1	44	13	-	5	17	15	17	11	48	5	82	45	x	-	-	1	-	1	-	x	x	-	-	-	-	-	-	-	-	-	19	305
		11H-5, 80-82	-	55	12	x	2	12	40	30	4	34	x	36	51	-	-	5	x	-	20	4	x	-	x	-	-	-	-	-	-	-	-	20	305
		11H-5, 91-93	7	79	7	x	8	15	19	4	10	17	x	79	49	12	4	-	x	-	2	3	-	-	-	-	-	-	-	-	-	-	-	19	315
		11H-5, 117-119	2	84	4	-	15	7	11	7	12	40	4	50	62	5	-	-	x	-	-	1	-	1	1	-	-	-	-	-	-	-	-	19	306
		11H-5, 120-122	2	77	4	-	3	9	17	19	3	33	21	58	47	-	x	2	1	-	2	1	1	3	1	-	-	-	-	-	-	-	-	22	304
		11H-5, 145-147	36	16	-	x	14	15	29	10	14	25	9	24	59	27	14	4	x	-	x	3	-	11	-	-	-	-	-	-	-	-	-	22	310
		11H-6, 9-10'	3	71	7	-	3	13	3	27	11	60	11	56	31	-	-	8	1	-	2	-	4	4	-	-	-	-	-	-	-	-	-	19	315
		11H-6, 19-20	2	59	9	-	5	20	10	20	5	49	26	32	28	2	1	20	1	-	2	-	8	6	-	-	-	-	-	-	x	x	-	23	305
		11H-6, 29-30	-	25	9	-	9	13	29	29	8	52	14	44	56	-	-	-	1	-	5	-	1	4	-	-	-	x	-	x	-	-	-	19	299
		11H-6, 39-40	-	53	3	1	9	15	52	37	6	45	20	-	76	-	-	2	-	-	2	2	1	3	-	2	-	-	-	x	-	-	-	18	329
		11H-6, 49-50	x	67	2	x	9	29	42	42	12	4	12	45	26	-	-	1	1	-	3	2	1	2	-	-	-	-	-	-	-	-	-	21	300
		11H-6, 59-60	1	62	52	x	4	9	63	3	6	2	4	-	96	1	-	3	5	-	6	1	-	-	2	-	-	x	-	x	-	-	-	22	320
		11H-6, 69-70	9	87	25	-	18	11	9	13	16	9	6	-	61	10	8	3	5	-	2	-	2	14	x	-	-	-	x	-	-	-	-	21	308
	MPl1	11H-6, 79-80	-	63	26	x	9	26	4	52	35	3	21	3	35	-	-	26	5	-	x	-	x	7	-	x	-	-	-	-	-	-	-	17	315
		11H-6, 90-91	-	93	31	-	8	30	1	43	24	x	22	-	33	-	-	17	1	-	1	1	x	3	x	2	x	x	-	-	-	-	-	21	310
		11H-6, 98-99	1	87	5	-	x	16	3	47	18	4	6	-	65	-	-	7	5	-	6	x	2	10	-	-	-	-	-	-	-	-	-	19	282
		11H-6, 108-109	-	97	28	x	8	18	58	35	9	-	13	-	25	-	-	3	x	-	1	x	x	3	1	-	1	-	-	-	-	-	-	19	300
		11H-6, 117-118	1	87	12	3	10	17	54	4	3	2	4	-	100	-	-	x	2	-	4	x	1	-	-	x	2	-	-	-	-	-	-	20	306
		11H-6, 124-126	29	56	11	-	3	19	29	9	4	x	14	-	84	34	15	-	1	-	x	1	-	x	x	-	-	-	-	-	-	-	-	18	309
l. Mio.	not zoned	11H-6, 128-129	-	7	3	1	10	27	34	28	20	1	21	1	14	3	1	1	2	-	-	-	-	3	-	-	-	-	-	-	-	-	-	17	177
		11H-6, 139-140	35	32	3	-	15	29	35	17	13	1	27	1	46	26	4	1	15	-	1	2	1	4	-	-	-	-	-	-	-	-	-	20	308
		11H-7, 8-10'	30	35	5	6	5	21	48	13	1	36	6	7	21	4	2	1	d	-	2	-	-	-	-	-	-	-	-	-	-	-	-	20	243
		11H-7, 40-42	3	4	1	1	2	4	3	8	2	4	11	1	-	-	-	-	-	-	-	-	-	-	-	-	-	-	-	-	-	-	-	12	44

Note: x = simple occurrence, but not represented in the 300 specimens counted.

ronment. The concurrence of planktonic foraminifers and ostracodes in the same samples representing the uppermost Messinian Lago Mare facies is problematic and indicates either reworking, contamination or temporary incursion of "Atlantic" water into a fully Lago Mare environment.

The isotopic composition of the concurring ostracodes and planktonic foraminifers at Hole 967A reflects a shared environment for at least a short interval, as also pointed out by Cita (1973a). In addition, the interval where the higher abundance of planktonic foraminifers associated with ostracodes is observed coincides with the low calcium carbonate peak between 121.6 and 122.4 m (Table 1; Fig. 4). Based on these observations, a temporary incursion of "Atlantic" water into a fully Lago Mare environment is the more reasonable explanation for the presence of planktonic foraminifers in sediment deposited before the Zanclean transgression.

The Zanclean transgression appears as a deep-sea flood extending to the distal part of the Eastern Mediterranean. The sedimentary expression of this event differs at the various sites, indicating a variety of situations that influenced the flood, which appears as a rapid rise of sea level with open marine conditions invading previously isolated and depressed ponds. The existence of sills results in the development of cyclically repeated anoxic conditions, as recorded in the Mediterranean drill holes. In other distal locations, however, oxygenation is good, as observed on the Eratosthenes Seamount and in the Pissouri section measured on western Cyprus (Orszag-Sperber and Rouchy, 1979; Cita et al., unpubl. data).

Repopulation of the Eastern Mediterranean by benthic biota (foraminifers) was gradual. Deep Atlantic taxa (*Parrelloides bradyi* and *P. robertsonianus*) appeared in correspondence with the termination of the *Sphaeroidinellopsis* acme event, as also reported by Wright (1980) and McKenzie et al. (1990). The occurrence of a negative reversal in the oxygen isotopic composition of the benthic foraminifers at the end of the *Sphaeroidinellopsis* acme event may represent a paleoceanographic reversal in the recovery of the Mediterranean to full marine conditions after the terminal flooding. A similar isotopic excursion in the Tyrrhenian Sea was interpreted as the result of a reorganization of the paleocirculation pattern in the Western Mediterranean with the initial opening of a new shallow connection to the Atlantic Ocean, which would become the site of the modern Straits of Gibraltar with continued headward erosion (McKenzie et al., 1990).

Peaks in the abundance of planktonic foraminiferal fauna observed in the Eastern Mediterranean drill sites recall those observed by Sprovieri (1992, 1993) in the central Mediterranean, which were interpreted as fluctuations forced by the precession astronomical cycles. Finally, the presence of Atlantic planktonic foraminiferal taxa, such as specimens belonging to the *Globorotalia menardii* group, at the boundary between the Zones MPl1 and MPl2, indicates that an efficient connection between the Atlantic Ocean and the Eastern Med-

Table 8. Distribution and species abundance of benthic foraminifers in Hole 969B.

Subseries	Pl. Foram. Zones	160-969B Core, section, interval (cm)	*C. carinata*	*G. subglobosa*	*B. subspinescens*	*C. italicus*	*O. stellatus*	*G. laevigatus*	*L. lobatula*	*N. turgida*	*P. alternans*	*C. helicinus*	*M. perparva*	*Q. bicarinata*	Species abundance	Sapropels
early Pliocene		11H-1, 31-33	-	-	-	-	vr	-	-	-	-	-	-	-	1	sap
	MPl2	11H-1, 100-102	-	-	-	-	r	r	-	-	-	-	-	r	3	
		11H-2, 30-32	-	r	-	-	r	r	-	-	-	r	r	r	6	
	MPl1	11H-2, 100-102	-	r	-	-	r	r	-	-	-	r	-	-	4	
		11H-3, 40-42	-	-	-	-	vr	-	-	-	-	-	-	-	1	sap
		11H-3, 130-132	-	-	-	-	vr	vr	-	-	-	-	-	-	2	
		11H-4, 40-42	-	-	-	-	vr	vr	-	-	-	-	-	-	2	
		11H-4, 120-122	-	-	-	-	r	r	-	-	-	r	-	-	3	
		11H-5, 3-5	-	-	-	-	-	-	-	-	-	-	-	-	0	sap
		11H-5, 7-9	-	-	-	-	-	-	-	-	-	-	-	-	0	sap
		11H-5, 30-32	r	-	vr	-	r	vr	-	-	-	-	-	-	4	
		11H-5, 50-52	-	-	vr	vr	r	vr	-	vr	-	-	-	-	5	
		11H-5, 70-72	-	r	-	-	r	r	-	-	-	-	-	-	3	
		11H-5, 80-82	-	vr	vr	-	vr	vr	-	vr	vr	-	-	-	6	
		11H-5, 91-93	-	-	-	-		-	-	-	-	-	-	-	0	sap
		11H-5, 117-119	-	r	-	-	r	-	vr	-	-	-	-	-	3	
		11H-5, 120-122	-	vr	vr	-	vr	-	-	-	-	-	-	-	3	
		11H-5, 145-147	-	-	-	-		-	-	-	-	-	-	-	0	sap
		11H-6, 9-10	-	-	-	vr	-	-	-	-	-	-	-	-	1	
		11H-6, 19-20	-	vr	vr	-	-	-	-	-	-	-	-	-	2	
		11H-6, 29-30	-	-	-	-	-	-	-	-	-	-	-	-	0	
		11H-6, 39-40	-	-	-	-	-	-	-	-	-	-	-	-	0	
		11H-6, 49-50	vr	-	-	-	-	-	-	-	-	-	-	-	1	
		11H-6, 59-60	-	-	-	-	-	-	-	-	-	-	-	-	0	sap
		11H-6, 69-70	-	-	-	-	-	-	-	-	-	-	-	-	0	sap
	MPl1	11H-6, 79-80	-	-	-	-	-	-	-	-	-	-	-	-	0	
		11H-6, 90-91	-	-	-	-	-	-	-	-	-	-	-	-	0	
		11H-6, 98-99	-	-	-	-	-	-	-	-	-	-	-	-	0	
		11H-6, 108-109	-	-	-	-	-	-	-	-	-	-	-	-	0	
		11H-6, 117-118	-	-	-	-	-	-	-	-	-	-	-	-	0	sap
		11H-6, 124-126	-	-	-	-	-	-	-	-	-	-	-	-	0	sap
l. Mio.	not Zoned	11H-6, 128-129	-	-	-	-	-	-	-	-	-	-	-	-	0	
		11H-6, 139-140	-	-	-	-	-	-	-	-	-	-	-	-	0	
		11H-7, 8-10	-	-	-	-	-	-	-	-	-	-	-	-	0	
		11H-7, 40-42	-	-	-	-	-	-	-	-	-	-	-	-	0	

Note: vr = very rare, r = rare.

iterranean Sea was re-established in this interval, as was previously determined from studies of a continuous Miocene/Pliocene boundary section from ODP Leg 107, Site 652 in the Tyrrhenian Sea (McKenzie et al., 1990).

Several lines of evidence suggest that, in late Messinian and early Zanclean times, the paleobathymetry of the Mediterranean Ridge drill site was deeper than that of the Eratosthenes Seamount drill site. First, the shallow-water, brackish Lago Mare biofacies is present in the more eastern location but was not recorded on the Mediterranean Ridge. Second, the lower Zanclean sediments on the Mediterranean Ridge are much poorer in benthic foraminifers and contain sapropels, whereas those on the Eratosthenes Seamount are well oxygenated and richer in bottom biota.

CONCLUSIONS

The Miocene/Pliocene boundary (Messinian/Zanclean boundary) as recorded in the ODP Leg 160 drill sites is probably coeval with that defined in Sicily at the type locality, where it has been carefully calibrated. It falls within the Gilbert Chron, five astronomical (precession) cycles in the magnetic reversal below the Thvera event, at the base of the foraminiferal Zone MPl1, with a numerical age of 5.32 Ma, using the time scale of Berggren et al. (1995).

The occurrence of Lago-Mare biofacies at the eastern end-member of the Mediterranean transect south of Cyprus and the strongly negative isotopic signature of the ostracode shells confirm the non-marine nature of the latest Messinian sediments laid down after the evaporitic episodes, as previously pointed out by Cita et al. (1978) and McKenzie and Ricchiuto (1978). In the Eastern Mediterranean, the deep-sea nature of the earliest Zanclean sediments is also confirmed, as is the progressive repopulation by the benthic communities with deep bathyal Atlantic taxa first appearing ~200,000 years after the initial flooding (Wright, 1980; McKenzie et al., 1990). A fully open deep-water connection to the Atlantic Ocean was established coincident with the MPl1/MPl2 boundary in both the Eastern and Western Mediterranean. In conclusion, from the Leg 160 data set depicting the event stratigraphy across the Miocene/Pliocene boundary

ODP Leg 160 - Hole 969B

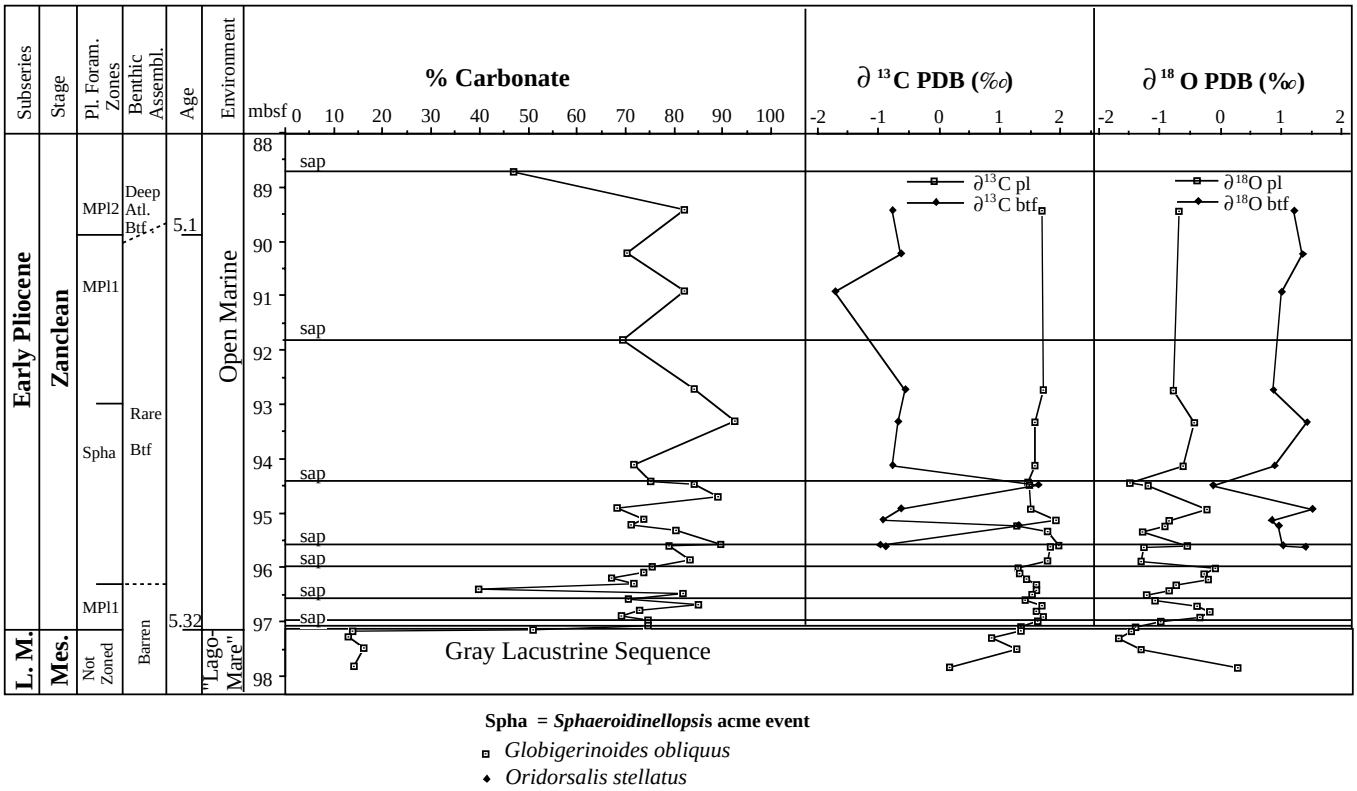

Figure 5. Summary of chemo- and biostratigraphy of the uppermost Miocene and lowermost Pliocene sediments of Hole 969B. Numerical age from Berggren et al. (1995). Horizontal lines (sap) indicate samples taken within sapropels.

ODP Leg 160 - Hole 969E

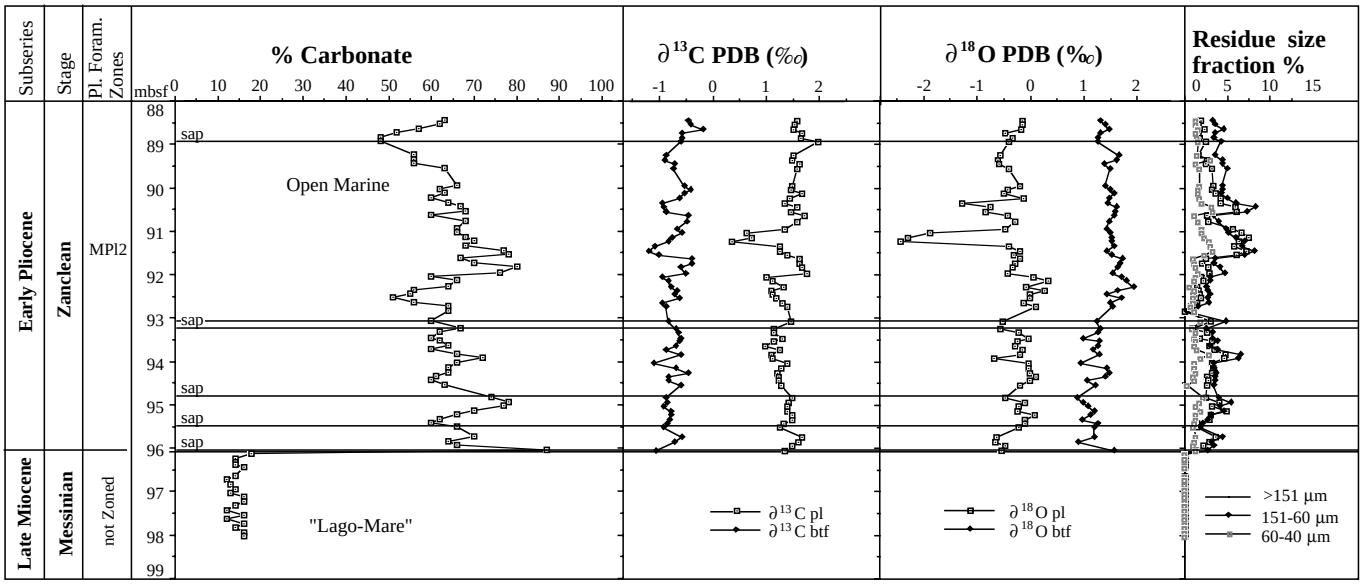

Figure 6. Summary of chemo- and biostratigraphy of the uppermost Miocene and lowermost Pliocene sediments of Hole 969E. Horizontal lines (sap) indicate samples taken within sapropels.

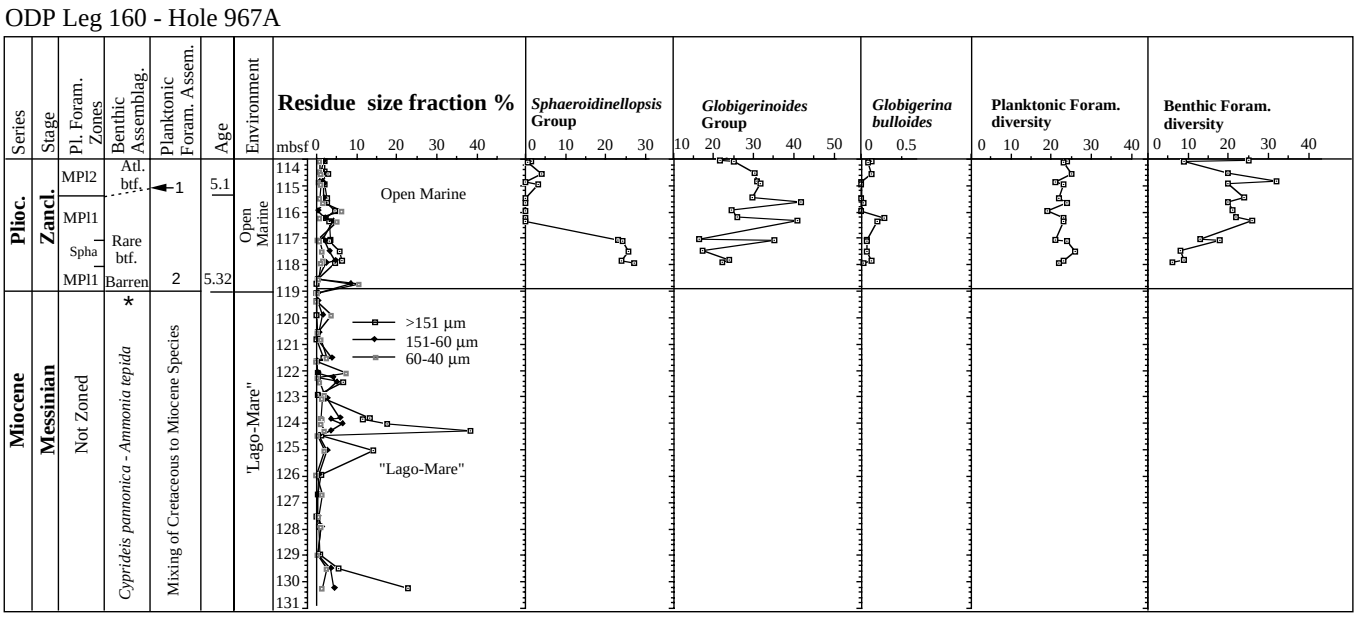

Figure 7. Plot of the abundance of *Sphaeroidinellopsis*, *Globigerinoides* groups, and *Globigerina bulloides* and planktonic and benthic foraminifer species abundance for Hole 967A.

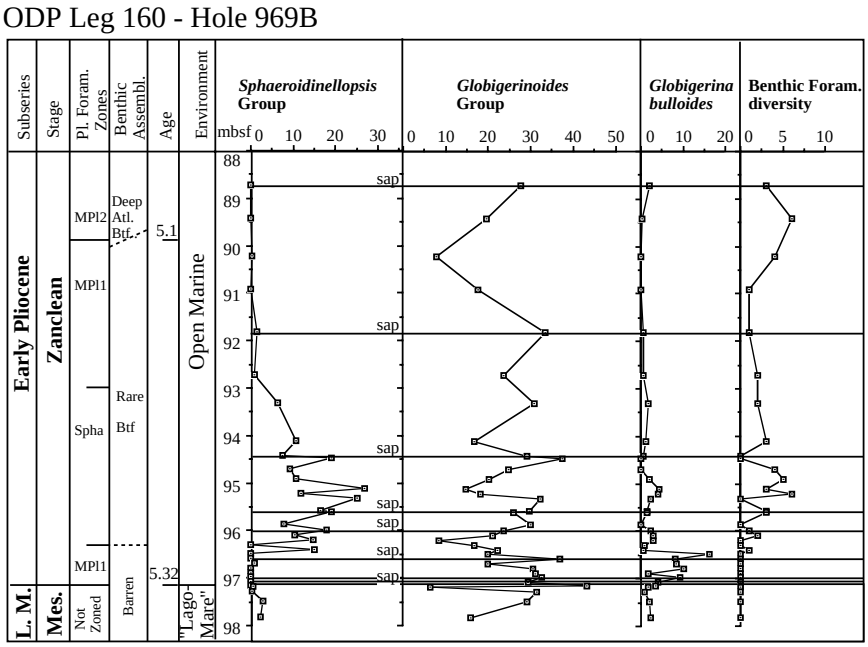

Figure 8. Plot of the abundance of *Sphaeroidinellopsis*, *Globigerinoides* groups, and *Globigerina bulloides* and benthic foraminifer species abundance for Hole 969B.

in the Eastern Mediterranean, the terminal Messinian flood and the earliest Pliocene paleoceanography appear to be similar and most likely synchronous throughout the entire Mediterranean Sea.

ACKNOWLEDGMENTS

We thank ODP for inviting Silvia Spezzaferri aboard on Leg 160 and providing the large number of samples. J. Terranes and S. Bernasconi are acknowledged for their assistance with the stable isotope measurements. The paper was helpfully reviewed by S. Iaccarino and R. Sprovieri. Financial support was given to Silvia Spezzaferri by the European Science Foundation and the Italian Consiglio Nazionale Ricerche (CNR).

REFERENCES

Benson, R.H., 1978. The paleoecology of the ostracodes of DSDP Leg 42A. *In* Hsü, K.J., Montadert, L., et al., *Init. Repts. DSDP,* 42 (Pt. 1): Washington (U.S. Govt. Printing Office), 777–787.

Benson, R.H., and Hodell, D.A., 1994. Comment on "A critical re-evaluation of the Miocene/Pliocene boundary as defined in the Mediterranean" by F.J. Hilgen and C.G. Langereis. *Earth Planet. Sci. Lett.*, 118:135–144.

Berggren, W.A., Hilgen, F.J., Langereis, C.G., Kent, D.V., Obradovich, J.D., Raffi, I., Raymo, M.E., and Shackleton, N.J., 1995. Late Neogene chro-

nology: new perspectives in high-resolution stratigraphy. *Geol. Soc. Am. Bull.*, 107:1272–1287.
Blechschmidt, G., Cita, M.B., Mazzei, R., and Salvatori, G. 1982. Stratigraphy of the Western Mediterranean and Southern Calabrian Ridges, Eastern Mediterranean. *Mar. Micropaleontol.*, 7:101–134.
Cita, M.B., 1973a. Inventory of biostratigraphical finding and problems. *In* Ryan, W.B.F., Hsü, K.J., et al., 1973. *Init. Repts. DSDP,* 13: Washington (U.S. Govt. Printing Office), 1045–1074.
————, 1973b. Pliocene biostratigraphy and chronostratigraphy. *In* Ryan, W.B.F., Hsü, K.J., et al. *Init. Repts. DSDP,* 13 (Pt. 2): Washington (U.S. Govt. Printing Office), 1343–1379.
————, 1975a. The Miocene/Pliocene boundary: history and definition. *In* Saito, T., and Burckle, L.H., (Eds.), *Late Neogene Epoch Boundaries.* Spec. Publ. Micropaleontol., 1–30.
————, 1975b. Studi sul Pliocene e gli strati di passaggio dal Miocene al Pliocene, VII. Planktonic foraminiferal biozonation of the Mediterranean Pliocene deep sea record: a revision. *Riv. Ital. Paleontol. Stratigr.,* 81:527–544.
Cita, M.B., and Gartner, S., 1973. Studi sul Pliocene e sugli strati al passaggio dal Miocene al Pliocene. IV. The stratotype Zanclean foraminiferal and nannofossil biostratigraphy. *Riv. Ital. Paleontol. Stratigr.,* 79:503–558.
Cita, M.B., Ramil, C., Wright, C., Ryan, W.B.F., and Longinelli, A., 1978. Messinian paleoenvironment. *In* Hsü, K., Montadert, L., et al., *Init. Repts. DSDP,* 42A: Washington (U.S. Govt. Printing Office), 1003–1036.
Cita, M.B., and Ryan, W.B.F., 1973. Timescale and general synthesis. *In* Ryan, W.B.F., Hsü, K.J., et al., *Init. Repts. DSDP*; 13: Washington (U.S. Govt. Printing Office), 1405–1416.
Cita, M.B., Vismara-Schilling, A., and Bossio, A., 1980. Stratigraphy and paleoenvironment of the Cuevas del Almazora Section (Vera Basin): a reinterpretation. *Riv. Ital. Paleontol. Stratigr.*, 86:215–240.
Craig, H., 1957. Isotopic standards for carbon and oxygen and correction factors for mass-spectrometric analysis of carbon dioxide. *Geochim. Cosmochim. Acta,* 12:133–149.
Emeis, K.-C., Robertson, A.H.F., Richter, C., et al., 1996. *Proc. ODP, Init. Repts.*, 160: College Station, TX (Ocean Drilling Program).
Hasegawa, S., Sprovieri, R., and Poluzzi, A., 1990. Quantitative analyses of benthic foraminiferal assemblages from Plio-Pleistocene sequences in the Tyrrhenian Sea, ODP Leg 107. *In* Kastens, K.A., Mascle, J., et al., 1990. *Proc. ODP, Sci. Results,* 107: College Station, TX (Ocean Drilling Program), 461–478.
Hilgen, F.J., 1991. Extension of the astronomically calibrated (polarity) time scale to the Miocene/Pliocene boundary. *Earth Planet. Sci. Lett.,* 107:349–368.
Hilgen, F.J., and Langereis, C., 1993. A critical re-evaluation of the Miocene/Pliocene boundary as defined in the Mediterranean. *Earth Planet. Sci. Lett.,* 118:167–179.
Hsü, K.J., Cita, M.B., and Ryan, W.B.F., 1973. The origin of the Mediterranean evaporites. *In* Ryan, W.B.F., Hsü, K.J., et al., *Init. Repts. DSDP,* 13 (Pt. 2): Washington (U.S. Govt. Printing Office), 1203–1231.
Hsü, K.J., Montadert, L., et al., 1978. *Init. Repts. DSDP,* 42 (Pt. 1): Washington (U.S. Govt. Printing Office).
Iaccarino, S., 1985. Mediterranean Miocene and Pliocene planktic foraminifera. *In* Bolli, H.M., Saunders, J.B., and Perch-Nielsen, K. (Eds.), *Plankton Stratigraphy:* Cambridge (Cambridge Univ. Press), 283–314.
McKenzie, J.A., Hodell, D.A., Mueller, P.A., and Mueller, D.W., 1988. Application of strontium isotopes to late Miocene-early Pliocene stratigraphy. *Geology,* 16:1022–1025.
McKenzie, J.A., and Ricchiuto, T.E., 1978. Stable isotopic investigation of carbonate samples related to the Messinian salinity crisis from DSDP Leg 42A, Mediterranean Sea. *In* Hsü, K., Montadert, L., et al., *Init. Repts. DSDP,* 42A: Washington (U.S. Govt. Printing Office), 651–655.
McKenzie, J.A., and Sprovieri, R., 1990. Paleoceanographic conditions following the earliest Pliocene flooding of the Tyrrhenian Sea. *In* Kastens, K.A., Mascle, J., et al., *Proc. ODP, Sci. Results*, 107: College Station, TX (Ocean Drilling Program), 405–414.
McKenzie, J.A., Sprovieri, R., and Channell, J.E.T., 1990. The terminal Messinian flood and earliest Pliocene paleoceanography in the Mediterranean: results from ODP Leg 107, Site 652, Tyrrhenian Sea. *Mem. Soc. Geol. Ital.*, 44:81–91.
Orszag-Sperber, F., and Rouchy, J.M., 1979. Le Miocene terminal et le Pliocene inferieur au Sud de Chypre. *V Sem. sur le Messinien, PIGC 117, Envenment Geologiques a la limite Miocene-Pliocene,* 40–47.
Premoli Silva, I., and Boersma, A., 1988. Atlantic Eocene planktonic foraminiferal historical biogeography and paleohydrographic indices. *Palaeogeogr., Palaeoclimatol., Palaeoecol.,* 67:315–356.
————, 1989. Atlantic Paleogene planktonic foraminiferal bioprovincial indices. *Mar. Micropaleontol.,* 14:357–371.
Premoli Silva, I., Castradori, D., and Spezzaferri, S., 1993. Calcareous nannofossil and planktonic foraminifer biostratigraphy of Hole 810C (Shatsky Rise, northwestern Pacific). *In* Natland, J.H., Storms, M.A., et al., *Proc. ODP, Sci. Results,* 132: College Station, TX (Ocean Drilling Program), 15–36.
Ryan, W.B.F., 1973. Geodynamic implications in the Messinian crisis of salinity. *In* Messinian events in the Mediterranean. *K. Nederl. Akad. Wetensh.*, 26–38.
Ryan, W.B.F., Hsü, K.J., et al., 1973. *Init. Repts. DSDP,* 13 (Pts. 1 and 2): Washington (U.S. Govt. Printing Office).
Spezzaferri, S., 1994. Planktonic foraminiferal biostratigraphy and taxonomy of the Oligocene and lower Miocene in the oceanic record: an overview. *Palaeontographica Ital.*, 81:1–187.
————, 1995. Planktonic foraminiferal paleoclimatic implications across the Oligocene-Miocene transition in the oceanic record (Atlantic, Indian and South Pacific). *Palaeogeogr., Palaeoclimatol., Palaeoecol.,* 114:43–74.
Sprovieri, R., 1992. Mediterranean Pliocene biochronology: a high resolution record based on quantitative planktonic foraminifera distribution. *Riv. Ital. Paleontol. Stratigr.,* 98:61–100.
————, 1993. Pliocene–early Pleistocene astronomically forced planktonic foraminifera abundance fluctuations and chronology of Mediterranean calcareous plankton bio-events. *Riv. Ital. Paleontol. Stratigr.,* 99:371–414.
Sprovieri, R., and Hasegawa, S., 1990. Plio-Pleistocene benthic foraminifer stratigraphic distribution in the deep-sea record of the Tyrrhenian Sea (ODP Leg 107). *In* Kastens, K.A., Mascle, J., et al., *Proc. ODP, Sci. Results*, 107: College Station, TX (Ocean Drilling Program), 429–459.
Wright, R., 1980. Benthic foraminiferal repopulation of the Mediterranean after the Messinian (late Miocene) event. *Palaeogeogr., Palaeoclimatol., Palaeoecol.*, 29:169–188.
Zijderveld, J.D.A., Zachariasse, W.J., Verhallen, P.J.J.M., and Hilgen, F.J., 1986. The age of the Miocene-Pliocene boundary. *Newsl. Stratigr.,* 16:169–181.

Date of initial receipt: 15 January 1997
Date of acceptance: 1 August 1997
Ms 160SR-026

APPENDIX

List of Species and Taxonomic Notes

Pliocene Planktonic Foraminifers

Planktonic and benthic foraminiferal species are listed in alphabetical order by genus. The generic and specific concepts and the species groups used by Iaccarino (1985) and Spezzaferri (1994) are retained herein, whenever possible.

Beella digitata (Brady, 1879) (= *Globigerina digitata* Brady)
Globigerina bulbosa LeRoy, 1944
Globigerina bulloides d'Orbigny, 1926
Globigerina falconensis Blow, 1959
"*Globigerina" venezuelana* Hedberg, 1937
Globigerinella obesa (Bolli, 1957) (= *Globorotalia obesa* Bolli)
Globigerinella siphonifera (d'Orbigny, 1839) (= *Hastigerina siphonifera* d'Orbigny)
Globigerinita glutinata (Egger, 1893) (= *Globigerina glutinata* Egger)
Globigerinita juvenilis (Bolli, 1957) (= *Globigerina juvenilis* Bolli)
Globigerinita uvula (Ehrenberg, 1861) (= *Pylodexia uvula* Ehrenberg)
Globigerinoides gomitulus (Seguenza, 1880) (= *Globigerina gomitulus* Seguenza)
Globigerinoides obliquus Bolli, 1957
Globigerinoides quadrilobatus (d'Orbigny, 1846) (= *Globigerina quadrilobata* d'Orbigny)
Globigerinoides ruber (d'Orbigny, 1839) (= *Globigerina rubra* d'Orbigny)

Globigerinoides sacculifer (Brady, 1877) (= *Globigerina sacculifera* Brady)
Globigerinoides trilobus (Reuss, 1850) (= *Globigerina triloba* Reuss)
Globorotalia margaritae Bolli and Bermudez, 1965
Globorotalia menardii (Parker, Jones, and Brady, 1865) (= *Rotalia menardii* Parker, Jones, and Brady)
Globorotalia scitula (Brady, 1882) (= *Pulvinulina scitula* Brady)
Neogloboquadrina acostaensis (Blow, 1959) (= *Globorotalia acostaensis* Blow)
Neogloboquadrina dutertrei (d'Orbigny, 1839) (= *Globigerina dutertrei* d'Orbigny)
Neogloboquadrina pachyderma (Ehrenberg, 1861) (= *Aristospira pachyderma* Ehrenberg)
Orbulina universa d'Orbigny, 1839
Sphaeroidinella dehiscens (Parker and Jones, 1865) (= *Sphaeroidina bulloides* d'Orbigny var. *dehiscens* Parker and Jones)
Sphaeroidinellopsis kochi (Caudri, 1934) (= *Globigerina kochi* Caudri)
Sphaeroidinellopsis subdehiscens Blow, 1969
Sphaeroidinellopsis seminulina (Schwager, 1866) (= *Globigerina seminulina* Schwager)
Tenuitella anfracta (Parker, 1967) (= *Globorotalia anfracta* Parker)
Turborotalita quinqueloba Natland, 1938 (= *Globigerina quinqueloba*, Natland)
Zeaglobigerina decoraperta (Takayanagi and Saito, 1962) (= *Globigerina decoraperta* Takayanagi and Saito)
Zeaglobigerina nepenthes (Todd, 1957) (= *Globigerina nepenthes* Todd). Small-sized specimens with smaller aperture than typical *Z. nepenthes* and resembling *Zeaglobigerina druryi* have been separated under *Z. nepenthes* group.
Zeaglobigerina woodi (Jenkins, 1960) (= *Globigerina woodi* Jenkins)
Streptochilus globigerum (Schwager, 1986) (= *Textilaria globigera* Schwager)

Planktonic Foraminifers Contained in the Messinian Sediments

The generic and specific concepts and the species groups are those used by Premoli Silva and Boersma (1988, 1989) and Spezzaferri (1994).

Acarinina bullbrooki (Bolli, 1957) (= *Globorotalia bullbrooki* Bolli)
Acarinina pentacamerata Subbotina, 1953
Acarinina soldadoensis (Brönnimann, 1952) (= *Globigerina soldadoensis* Brönnimann)
Cassigerinella chipolensis (Cushman and Ponton, 1932) (= *Cassidulina chipolensis* Cushman and Ponton)
Chiloguembelina cubensis (Palmer, 1934) (= *Guembelina cubensis* Palmer).
Dentoglobigerina galavisi (Bermudez, 1961) (= *Globigerina galavisi* Bermudez)
"Globigerina" ciperoensis Bolli, 1957
Globoquadrina dehiscens (Chapman, Parr and Collins, 1934) (= *Globorotalia dehiscens* Chapman, Parr and Collins)
Paragloborotalia pseudokugleri (Blow, 1969) (= *Globorotalia pseudokugleri* Blow)
Paragloborotalia acrostoma (Wezel, 1966) (= *Globorotalia acrostoma* Wezel)
Paragloborotalia kugleri (Bolli, 1957) (= *Globorotalia kugleri* Bolli)
Paragloborotalia opima (Bolli, 1957) (= *Globorotalia opima opima* Bolli)
Planorotalites pseudoscitulus (Glaessner, 1937) (= *Globorotalia pseudoscitula* Glaessner)
Praeorbulina transitoria (Blow, 1956) (= *Globigerinoides transitoria* Blow)
Subbotina angiporoides angiporoides (Hornibrook, 1965) (= *Globigerina angiporoides* Hornibrook)
Subbotina utilisindex (Jenkins and Orr, 1973) (= *Globigerina utilisindex* Jenkins and Orr)
Turborotalia griffinae Blow, 1979
Zeaglobigerina ampliapertura (Bolli, 1957) (= *Globigerina ampliapertura* Bolli)

Benthic Foraminifers

Generic and specific concepts of Sprovieri and Hasegawa (1990) and Hasegawa et al. (1990) are retained here.

Anomalinoides helicinus (Costa, 1857) (= *Nonionina helicina* Costa)
Astrononion stelligerum (d'Orbigny, 1839) (= *Nonionina stelligera* d'Orbigny)
Bigenerina nodosaria d'Orbigny, 1826
Bolivina subspinescens Cushman, 1922
Brizalina punctata d'Orbigny, 1839
Brizalina dilatata (Reuss, 1850) (= *Bolivina dilatata* Reuss)
Cibicidoides italicus (Di Napoli, 1952) (= *Cibicides italicus* Di Napoli)
Cibicidoides ornatus (Costa, 1856) (= *Nonionina ornata* Costa)
Cibicidoides pachyderma (Rzehak, 1866) (= *Truncatulina pachyderma* Rzehak)
Cibicidoides ungerianus (d'Orbigny, 1846) (= *Rotalina ungeriana* d'Orbigny)
Cribrobulimina serpens Seguenza emend. Sellii, 1941
Cylindroclavulina rudis (Costa, 1855) (= *Glandulina rudis* Costa)
Dentalina leguminiformis (Batsch, 1791) (= *Nautilus leguminiformis* Batsch)
*Eggerella brady*i (Cushman, 1911) (= *Verneuilina brady* Cushman)
Globocassidulina subglobosa (Brady, 1881) (= *Cassidulina globosa* Brady)
Gyroidina soldanii (d'Orbigny, 1826) (= *Rotalina soldanii* d'Orbigny)
Gyroidinoides laevigataus (d'Orbigny 1826) (= *Gyroidina laevigata* d'Orbigny)
Karreriella bradyi (Cushman, 1911) (= *Gaudryna brady* Cushman)
Lagena clavata (d'Orbigny, 1846) (*Oolina clavata* d'Orbigny)
Lenticulina cultrata (de Montfort, 1808) (= *Robulus cultratus* de Montfort)
Lenticulina gibba (d'Orbigny, 1839) (= *Cristellaria gibba* d'Orbigny)
Lenticulina inornata (d'Orbigny, 1846) (= *Robulina inornata* d'Orbigny)
Lenticulina rotulata (Lamark, 1804) (= *Lenticulites rotulata* Lamark)
Lobatula lobatula (Walter and Jacob, 1798) (= *Nautilus lobatulus* Walter and Jacob 1798)
Martinottiella communis (d'Orbigny, 1826) (= *Clavulina communis* d'Orbigny)
Martinottiella perparva (Cushman, 1936) (= *Listerella communis* (d'Orbigny) var. *perparva* Cushman)
Oolina faveolata (Seguenza, 1862) (= *Orbulina faveolata* Seguenza)
Oridorsalis stellatus (Silvestri, 1898) (= *Truncatulina tenera* Brady var. *stellata* Silvestri)
Parrelloides bradyi (Trauth, 1918) -*Parrelloides robertsonianus* (Brady, 1881). According with Sprovieri and Hasegawa (1990) these two forms are here considered as macrospheric and microspheric forms of the same species. However, in the range chart the two morphotypes are separate because of the distinctive characters of *P. bradyi* displaying smaller size, reduced numbers of chambers in the last whorl and oblique sutures on the spiral side.
Planulina ariminensis d'Orbigny, 1826
Pleurostomella alternans Schwager, 1866
Pseudoparrella exigua Conato, 1964
Pullenia bulloides (d'Orbigny, 1846) (= *Nonionina bulloides* d'Orbigny)
Pullenia osloensis Feyling-Hanssen, 1954
Pullenia quadriloba (Reuss, 1851) (= *Nonionina quadriloba* Reuss)
Pullenia quinqueloba (Reuss, 1851) (= *Nonionina quadriloba* Reuss)
Pullenia salisbury Stewart and Stewart, 1930
Quinqueloculina bicarinata d'Orbigny, 1826
Quinqueloculina laevigata. d'Orbigny, 1949
Quinqueloculina viennensis J. and Y. Le Calvez, 1958
Sigmoilinita tenuis (Czjek, 1848) (= *Quinqueloculina tenuis* Czjek)
Sigmoilopsis schlumbergeri (Silvestri, 1904) (= *Sigmoilina schlumbergeri* Silvestri)
Siphonina planoconvexa (Silvestri, 1898) (= *Truncatulina reticulata* (Czjek) var. *planoconvexa* Silvestri)
Siphonina reticulata (Czjek, 1848) (= *Rotalina reticulata* Czjek)
Sphaeroidina bulloides d'Orbigny, 1826
Stilostomella antillea (Cushman, 1923) (= *Nodosaria antillea* Cushman)
Stilostomella hispida (d'Orbigny) (= *Nodosaria hispida* d'Orbigny)
Stilostomella monilis (Silvestri, 1872) (= *Nodosaria monilis* Silvestri)
Uvigerina peregrina Cushman, 1923
Uvigerina pygmaea d'Orbigny, 1826
Uvigerina rutila Cushman and Todd, 1941
Vaginulinopsis carinata (Silvestri, 1904) (= *Vaginulinopsis inversa* (Costa) var. *carinata* Silvestri
Valvulineria marmorea Conato, 1964
Vulvulina pennatula (Batsch, 1791) (= *Nautilus pennatulus* Batsch)

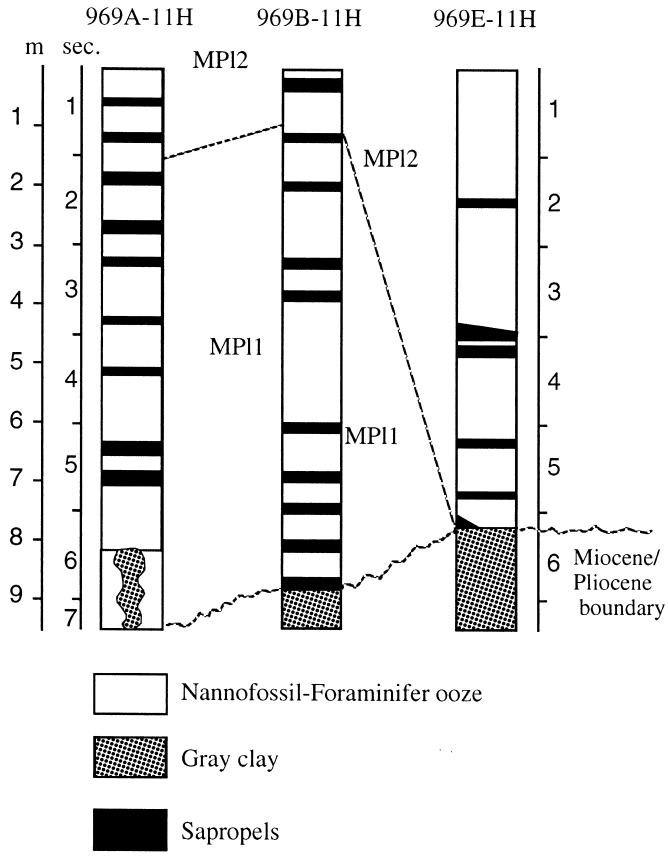

Figure 9. Correlation of Cores 160-969A-11H, 969B-11H and 969E-11H. Note that the most complete sequence is from Hole 969B.

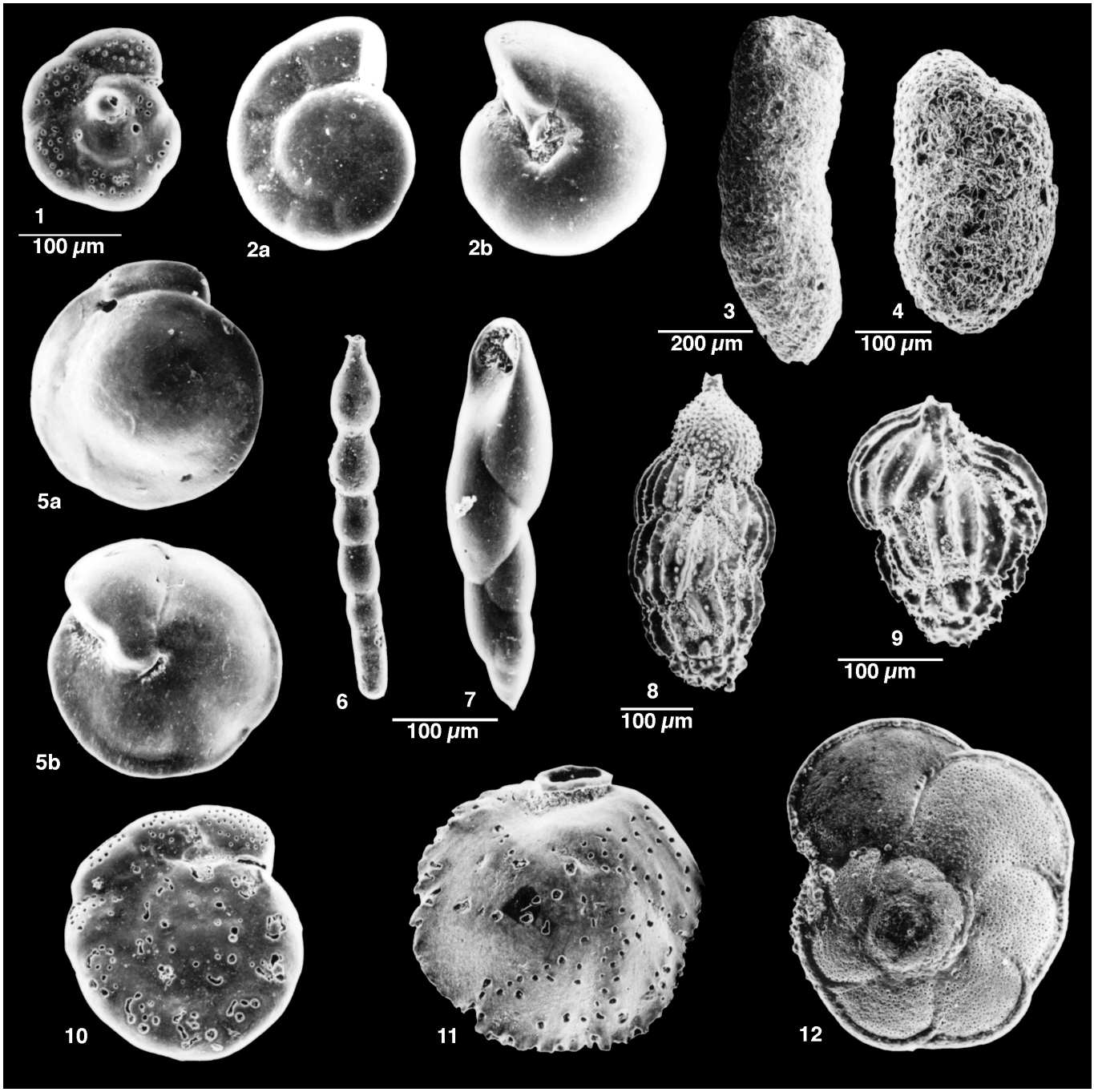

Plate 1. Benthic and the planktonic foraminifer *Globorotalia menardii* from the Eastern Mediterranean. **1.** *Parrelloides bradyi* (Trauth), Sample 160-967A-12H-1, 65–67 cm. **2a–b.** *Gyroidinoides laevigatus* (d'Orbigny), Sample 160-967A-12H-1, 65–67 cm. **3.** *Martinottiella perparva* (Cushman), Sample 160-167A-13H-2, 77–79 cm. **4.** *Martinottiella communis* (d'Orbigny), Sample 160-967A-12H-1, 65–67 cm. **5a–b.** *Oridorsalis stellatus* (Silvestri), Sample 160-967A-12H-1, 65–67 cm. **6.** *Stilostomella antillea* (Cushman), Sample 160-967A-12H-1, 65–67 cm. **7.** *Pleurostomella alternans* Schwager, Sample 160-967A-12H-1, 65–67 cm. **8**. *Uvigerina pygmaea* d'Orbigny, Sample 160-967A-12H-1, 65–67 cm. **9.** *Uvigerina* cf. *peregrina* Cushman, Sample 160-967A-12H-1, 65–67 cm. **10.** *Parrelloides robertsonianus* (Brady), Sample 160-967A-12H-1, 65–67 cm. **11.** *Siphonina reticulata* (Czjek), Sample 160-967A-12H-1, 65–67 cm. **12.** *Globorotalia menardii* (Parker, Jones, and Brady), Sample 160-967A-13H-2, 35–37 cm. (a = spiral view, b = umbilical view). Figures 1, 2, 5, 6, 7, 10, 11 and 12 are at the same magnification.

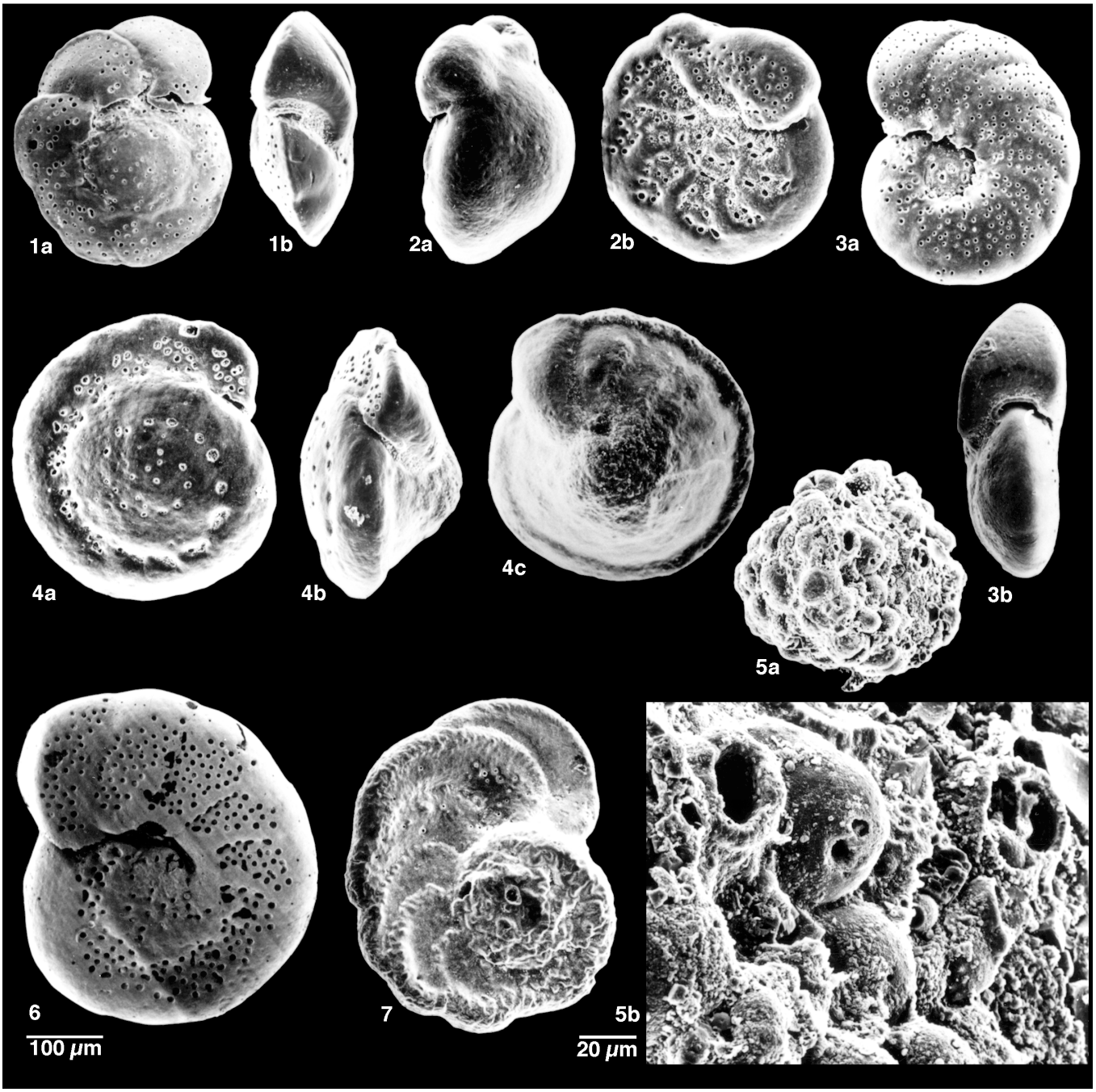

Plate 2. Benthic foraminifer from the Eastern Mediterranean. **1a–b.** *Cibicidoides ungerianus* (d'Orbigny), Sample 160-167A-13H-2, 77–79 cm. **2a–b.** *Cibicidoides italicus* (Di Napoli), Sample 160-967A-12H-1, 65–67 cm, a = side view and b = umbilical view. **3a–b**. *Anomalinoides helicinus* (Costa), Sample 160-967A-12H-1, 65–67 cm. **4a–c.** *Cibicidoides pachyderma* (Rzehak), Sample 160-967A-12H-1, 65–67 cm. **5a–b.** *Cylindroclavulina rudis* (Costa), Sample 160-67A-12H-5, 61–63 cm, b, detail of the wall texture. **6.** *Cibicidoides ornatus* (Costa), Sample 160-967A-12H-5, 61–63 cm, spiral view. **7.** *Planulina ariminensis* d'Orbigny, Sample 160-967A-12H-1, 65–67 cm, spiral view. (a = spiral view, b = side view, c = umbilical view). All specimens except 5b are at the same magnification.

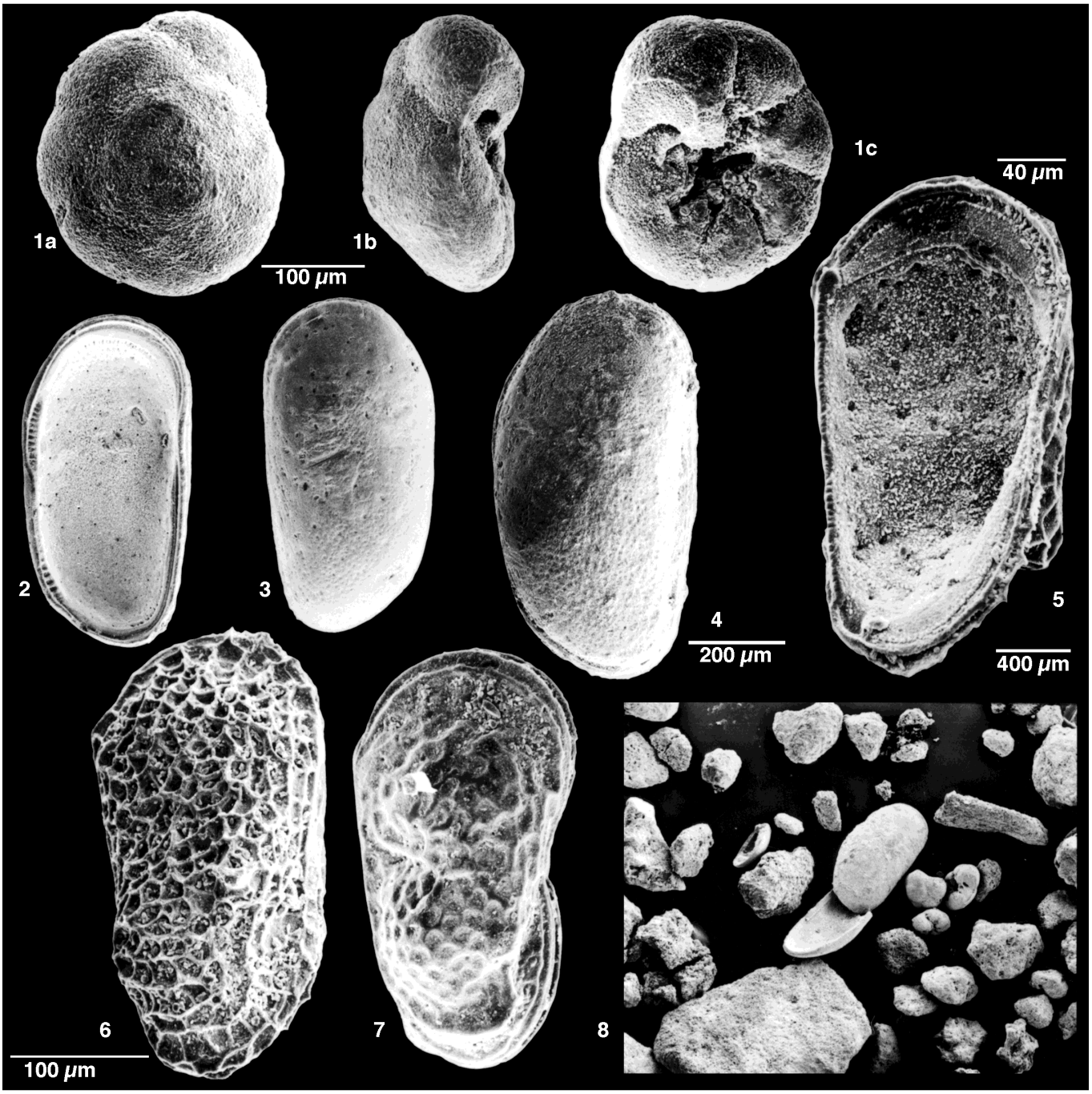

Plate 3. Lago Mare fauna and facies in the Eastern Mediterranean. **1a–c.** *Ammonia tepida* Cushman. a = spiral view, b = side view, c = umbilical view. **2.** *Cyprideis pannonica* (Mehes), Sample 160-967A-13H-7, 12–14 cm. **3.** *Cyprideis pannonica* (Mehes), Sample 160-967A-14H-1, 50–52 cm. **4.** *Cyprideis pannonica* (Mehes), specimen with the valves still attached, Sample 160-967A-13H-7, 12–14 cm. **5.** *Loxoconca diaffarovi* Schneider, Sample 160-967A-13H-4, 109–111 cm. **6.** *Loxoconca diaffarovi* Schneider, specimen with the valves still attached, Sample 160-967A-13H-4, 109–111 cm. **7.** *Loxoconca diaffarovi* Schneider, specimen with the valves still attached, Sample 160-967A-13H-4, 109–111 cm. **8.** Lago Mare facies. Note the specimens of *C. pannonica* and *A. tepida*, Sample 160-967A-14X-2, 21–23 cm. Figures 2, 3, 4, 6, and 7 are at the same magnification.

Prior Chapter Contents Next Chapter